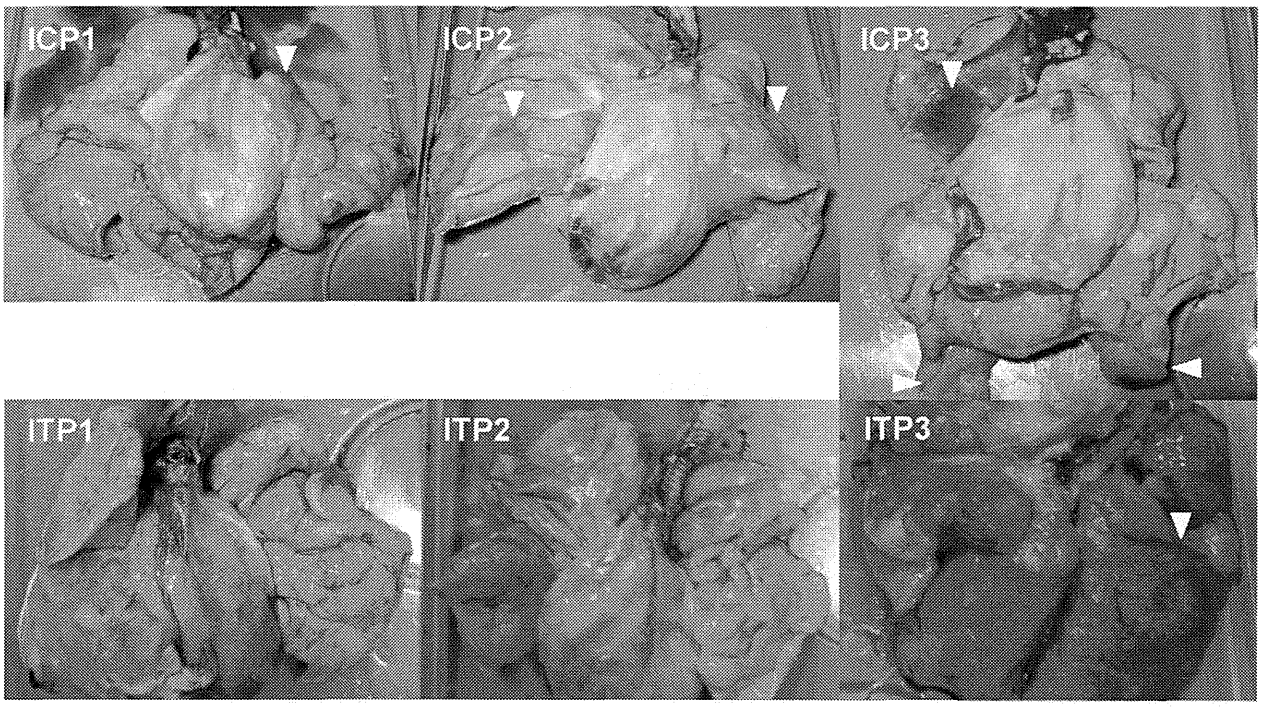

Figure 8. Gross pathological changes of the lungs of immunosuppressed and peramivir-treated macaques infected with VN3040. Immunosuppressed macaques were treated with control antibodies (ICP1–ICP3) or MAb ch61 (ITP1–ITP3) together with peramivir. Macaques ICP1, ICP3, and ITP3 were autopsied 5 days, 4 days, and 3 days after virus infection, respectively. The other macaques survived during the observation period and were autopsied 7 days after virus infection. Dark red lesions indicated by white arrowheads show macroscopic congestion.
doi:10.1371/journal.ppat.1004192.g008

Gross pathology and histopathology of macaques infected with H5N1 HPAI virus

To evaluate the progression of disease after the antibody treatment, we examined the lung pathology of the macaques subjected to autopsy. Macroscopically, dark red areas representing inflammation and congestion were larger in the lungs of control immunocompetent macaques (C1–C3) than in the lungs of two immunocompetent macaques treated with MAb ch61 (T1 and T2) (Fig. 6). The dark red area was larger in the lung of T3 than in the lungs of T1 and T2. These findings were concordant with virus titers in the lungs collected at autopsy (Table 2). In immunosuppressed macaques treated with control antibodies (IC1–IC3), the macroscopic lesions with inflammation, hemorrhage, and congestion in the lungs were much smaller than those in the lungs of immunocompetent macaques (C1–C3) (Figs. 6, 7). In immunosuppressed macaques treated with MAb ch61 (IT1–IT5), the reddish lesions were smaller than those in control macaques (IC1–IC3) (Fig. 7). In particular, macroscopic inflammation in IT5 was observed only around the central bronchus. In immunosuppressed macaques also treated with peramivir, macroscopic reddish lesions were smaller than those in immunocompetent and immunosuppressed macaques treated without peramivir (Figs. 6–8). The lung of ICP3, which died on day 4 after virus infection, had dark red, edematous lesions.

We then examined histological changes of the lungs collected from the infected macaques (Figs. 9–11). Severe pneumonia reducing air space was seen in a control immunocompetent macaque (C2) and a macaque treated with MAb ch61 (T1) (Figs. 9A, B). In high magnification images, lymphoid and neutrophilic infiltration, thickened alveolar walls, and alveolar edema were observed (Figs. 9C, D). The other macaques (C2, T2, and T3) euthanized on day 7 showed similar histological changes (data not shown). In immunohistochemical staining for the influenza virus antigens, NP-positive cells were widely distributed and accumulated focally in the lung of the control macaque 7 days after virus infection (Fig. 9E). By contrast, NP-positive cells were seen but did not accumulate in the MAb ch61-treated macaque (Fig. 9F). Reduced numbers of NP-positive cells were also seen in the lungs of the other treated macaques (T2 and T3) (data not shown).

In macaques under the immunosuppressed condition, lymphoid infiltration was very mild compared with immunocompetent macaques. In the lung tissue obtained from a control macaque (IC3) at 4 days after virus infection, pulmonary edema was seen in the alveoli, resulting in loss of air space (Figs. 10A, C). In a macaque treated with MAb ch61 (IT2), the air space was decreased and alveolar septa were thickened in part, but the air content was still preserved (Figs. 10B, D). NP-positive cells were seen in the alveolar epithelium of the control macaque more frequently than in that of the MAb ch61-treated macaque (Figs. 10E, F). The cuboidal epithelial cells positive for the NP antigen were type II alveolar epithelial cells. Less severe histological changes and virus infection were also seen in the other treated macaques (IT1 and IT3) compared with the control macaques (data not shown). These differences in the histological changes and frequencies of NP-positive cells between control and MAb ch61-treated macaques were also seen in the macaques treated together with peramivir (Fig. 11).

Discussion

Current strategies for the control of influenza include vaccination and antiviral drug treatment. Neuraminidase inhibitors have been used for H5N1 HPAI virus infection in humans as well as

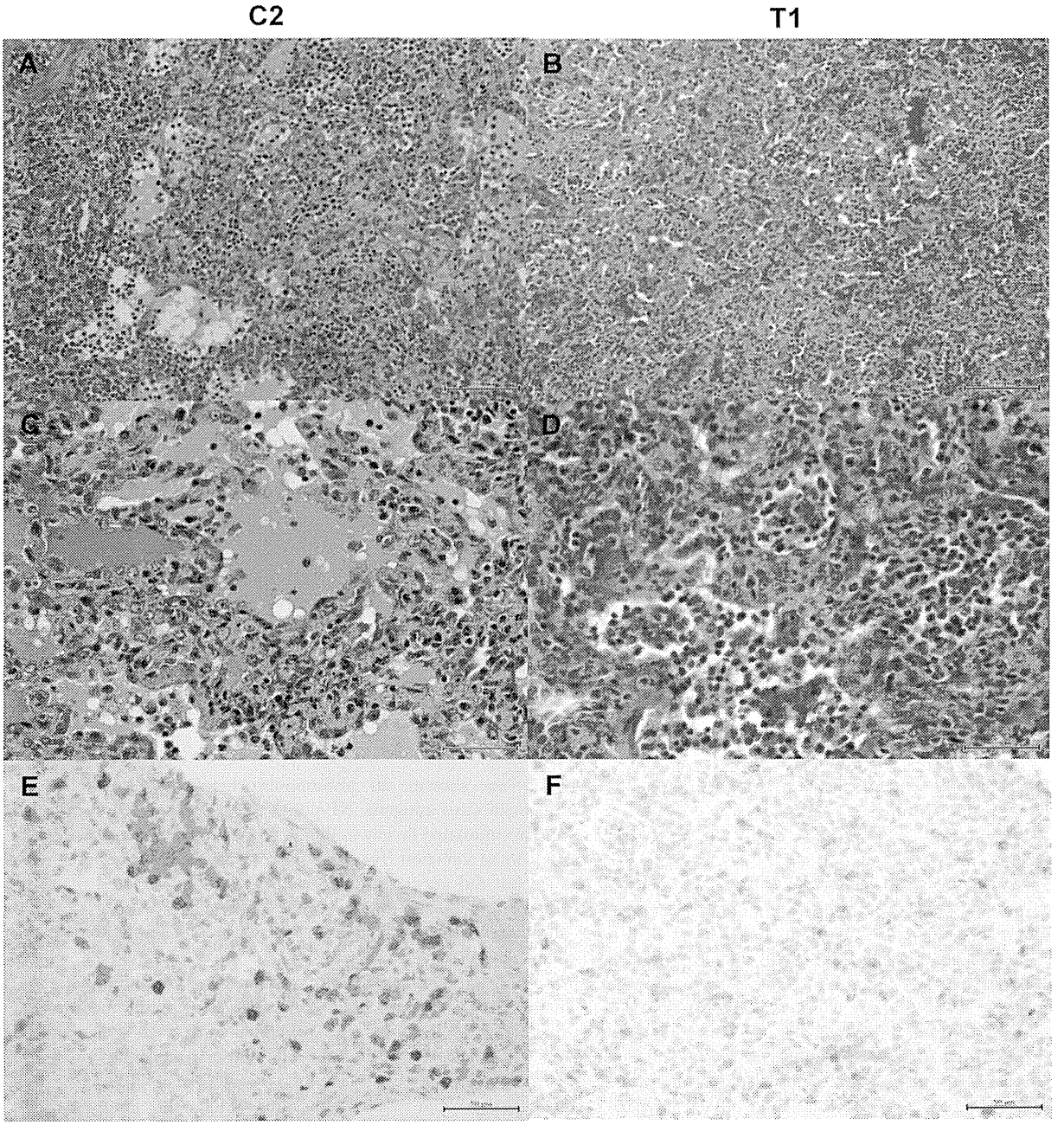

Figure 9. Histological analysis of pneumonia and distribution of viral antigens in immunocompetent macaques infected with VN3040. Tissues were collected from macaques injected with control antibodies (C2) (A, C, E) or MAb ch61 (T1) (B, D, F) on day 7 after virus infection. A, B: low magnification of hematoxylin and eosin (H & E) staining (bar: 100 μm). C, D: high magnification of H & E staining (bar: 50 μm). E, F: sections stained with anti-NP serum (bar: 50 μm).
doi:10.1371/journal.ppat.1004192.g009

seasonal influenza caused by viruses of the H1 and H3 HA subtypes. However, the efficacy of the neuraminidase inhibitors on the human H5N1 infections is unclear due to the inevitable lack of adequate control studies. Moreover, drug-resistant H5N1 viruses were indeed detected in patients [40,41] and, importantly, H5N1 viruses with reduced sensitivity to neuraminidase inhibitors were also isolated from chickens in the endemic area [42]. Thus, alternative strategies for prophylaxis and treatment need to be developed for pandemic preparedness against the H5N1 influenza virus.

Passive transfer of neutralizing antibodies may provide an alternative strategy for both prophylaxis and treatment of pandemic influenza. It was reported that an H5N1 HPAI virus-infected patient recovered after treatment with convalescent plasma, suggesting that passive immunotherapy may be a promising option for the treatment of H5N1 HPAI virus infection [43]. The efficacy of mouse MAbs specific for H5 HAs been evaluated in a mouse model with promising results for both treatments and prophylaxis [44,45]. However, for clinical use, induction of anti-mouse MAb-specific antibody responses should reduce the neutralizing capacity of given MAbs and also limit the repeated use of mouse antibodies. Thus, passive immunotherapy with human or humanized MAbs has also been tested in mouse

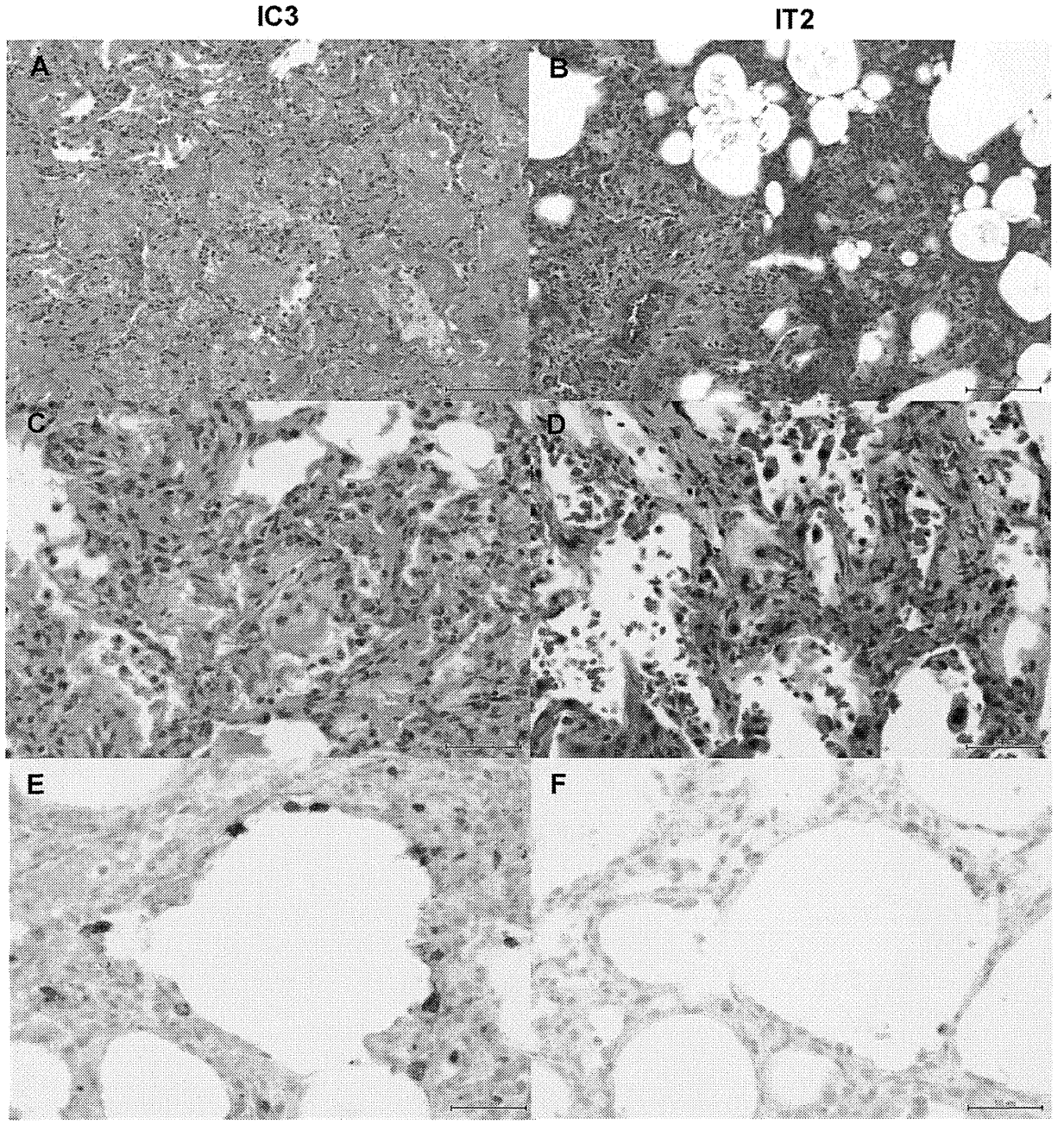

Figure 10. Histological analysis of pneumonia and distribution of viral antigens in immunosuppressed macaques infected with VN3040. Tissues were collected from macaques injected with control antibodies (IC3) (A, C, E) or MAb ch61 (IT2) (B, D, F) on days 4 and 7 after virus infection, respectively. Other details are the same as the legend of Figure 9.
doi:10.1371/journal.ppat.1004192.g010

and ferret models [46–49]. Nevertheless, the protective potential of anti-H5 MAbs remained to be elucidated in a nonhuman primate model of H5N1 HPAI virus infection.

To help develop a clinical antibody therapy, we also generated a human-mouse chimeric monoclonal antibody (MAb ch61) that showed strong neutralizing activity against H5N1 HPAI viruses isolated from humans and evaluated its protective potential in animal models. In particular, we used a cynomolgus macaque model, which simulates the H5N1 HPAI virus infection of humans more faithfully and thus has been used as an animal model for vaccine and pathogenesis studies on influenza virus infection [50]. We found that treatment with MAb ch61 reduced viral loads and partially protected macaques from lethal infection with the H5N1 HPAI virus. It was noteworthy that the protective effect was more prominent in immunosuppressed macaques, which might provide a model of protection against severe clinical disease in immunocompromised patients. Thus, this proof of concept study provides the first evidence that antibody therapy may have beneficial effects in clinical cases of H5N1 HPAI virus infection in humans. Importantly, however, mutant viruses escaping from neutralization by MAb ch61 were recovered from some of the macaques treated with MAb ch61 alone and became predominant by 7 days after infection, whereas reduced virus replication upon treatment with MAb ch61 was observed in most of the treated macaques

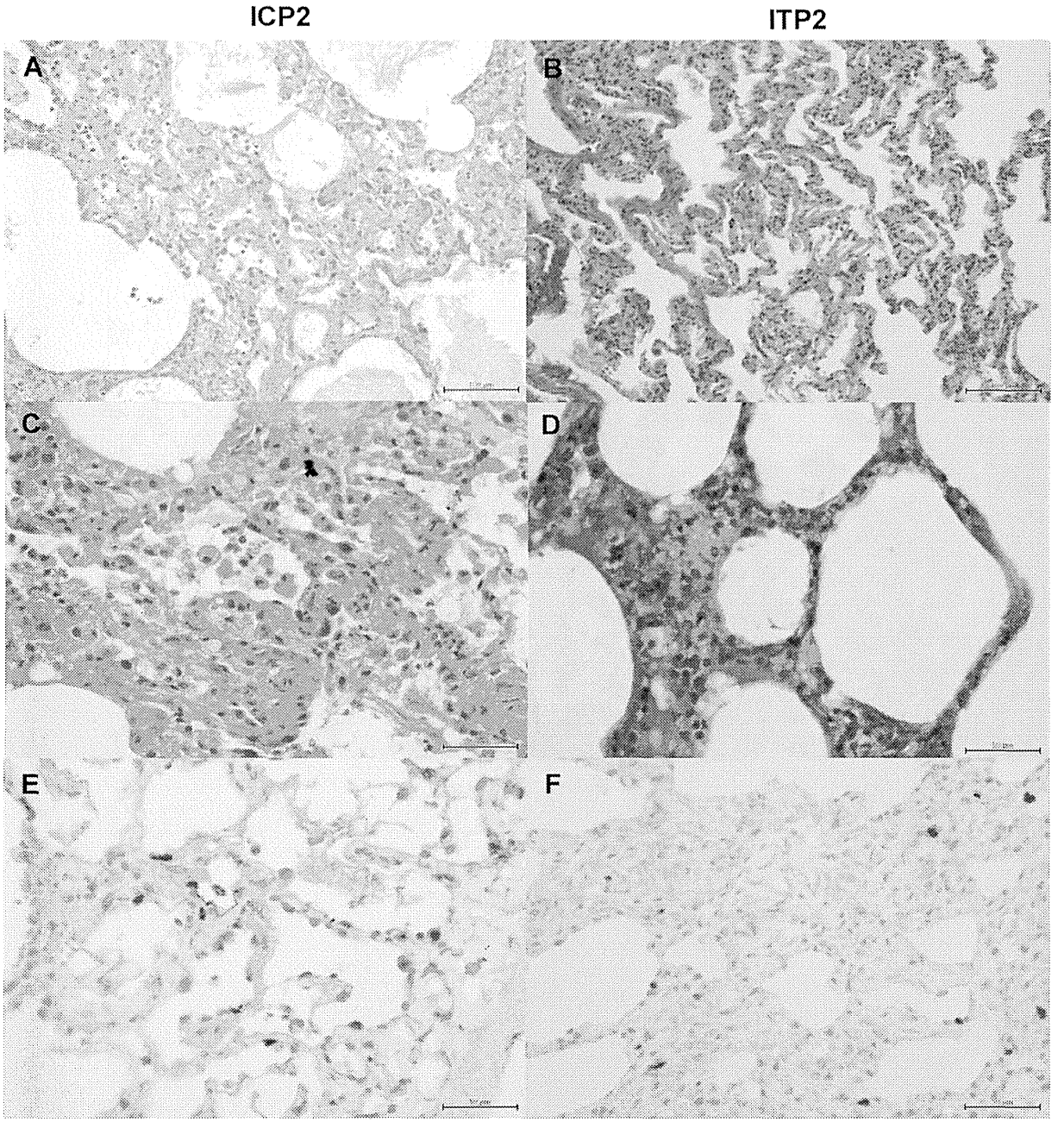

Figure 11. Histological analysis of pneumonia and distribution of viral antigens in immunosuppressed and peramivir-treated macaques infected with VN3040. Tissues were collected from macaques treated with peramivir and injected with control antibodies (ICP2) (A, C, E) or MAb ch61 (ITP2) (B, D, F) on day 7 after virus infection. Other details are the same as the legend of Figure 9.
doi:10.1371/journal.ppat.1004192.g011

during the initial phase of infection. These results suggest that, as was shown in a mouse model of H5N1 HPAI virus infection [51], combination therapy using two different MAbs might be needed to prevent the generation of escape mutants and would likely be more beneficial.

Taken together, the results obtained in the present study demonstrated that the therapeutic use of anti-H5 neutralizing MAb ch61 resulted in reduced viral loads and improved protection in a nonhuman primate model of lethal H5N1 virus infection. In addition, it was also shown that combination therapy with the antiviral drug provided better protection and reduced the emergence of escape mutants. Combination therapy with other antibodies recognizing different epitopes may also attenuate symptoms and prevent the selection of escape mutants.

Supporting Information

Figure S1 The number of white blood cells in macaques treated with immunosuppressive agents. The macaques were administered CP intravenously on days −7, −5, −3, −1 and 0 and CA intragastrically from day −7 to day 6 (A, B). A control group was administered saline intravenously and intragastrically (C). The macaques were injected intravenously with control MAbs (orange)

and MAb ch61 (blue). Macaques in (C) were injected with peramivir intravenously from day 1 to day 5 in addition to MAbs. Blood was collected on the indicated days. The number of white blood cells (WBC) was counted with a microscope and hemocytometer.
(TIFF)

Figure S2 Body temperatures of immunocompetent macaques treated with MAbs after infection with VN3040. Macaques were infected with VN3040 (3×10^6 PFU) on day 0. The macaques were injected intravenously with control MAbs (C1–C3, orange) or anti-H5 MAb ch61 (T1–T3, blue) on days 1 and 3. Depression of temperature was induced once a day by anesthesia.
(TIFF)

Figure S3 Body temperatures of immunocompromised macaques treated with MAbs after infection with VN3040. Macaques were pretreated with CP intravenously and with CA intragastrically. Thereafter, they were infected with VN3040 (3×10^6 PFU) on day 0. The macaques were injected intravenously with control MAbs (IC1–IC3, orange) or anti-H5 MAb ch61 (IT1–IT5, blue) on days 1 and 3. Depression of temperature was induced once a day by anesthesia.
(TIFF)

Figure S4 Body temperatures of immunocompromised macaques treated with MAbs and peramivir after infection with VN3040. Macaques were pretreated with CP intravenously and with CA intragastrically. Thereafter, they were infected with VN3040 (3×10^6 PFU) on day 0. The macaques were injected intravenously with control MAbs (ICP1–ICP3, orange) or anti-H5 MAb ch61 (ITP1–ITP3, blue) on days 1 and 3, and with peramivir on days 1 to 5. Depression of temperature once a day was induced by anesthesia.
(TIFF)

Figure S5 Cytokine patterns in the sera of macaques after infection with VN3040. Cytokine concentrations in the serum samples were measured as described in the Materials and Methods section. Left column: immunocompetent macaques (Exp. #1), middle column: immunosuppressed macaques (Exp. #2), right column: immunosuppressed macaques treated with peramivir (Exp. #3).
(PDF)

Figure S6 Cytokine patterns in the lungs of macaques after infection with VN3040. Cytokine concentrations in the lung tissue homogenates were measured as described in the Materials and Methods section. Left column: immunocompetent macaques (Exp. #1), middle column: immunosuppressed macaques (Exp. #2), right column: immunosuppressed macaques treated with peramivir (Exp. #3).
(PDF)

Table S1 Clinical scoring used in this study. Animals were monitored during the study to be clinically scored.
(DOCX)

Acknowledgments

We thank Kazumasa Yokoyama, Noriko Ikeda, Ayaka Yokoyama, and Aiko Ohnuma (Hokkaido University Research Center for Zoonosis Control) for helpful suggestions or technical assistance with the production of MAbs, and Kim Barrymore for editing the manuscript.

Author Contributions

Conceived and designed the experiments: YI RY KO AT. Performed the experiments: YI RY SS MH HIshig MN VLP HIshid MA NK YM TH MO YS HM MIs. Analyzed the data: YI RY MIg AT. Contributed reagents/materials/analysis tools: MK HT HK MIt LQM YK YS. Wrote the paper: YI RY AT.

References

1. Webster RG, Bean WJ, Gorman OT, Chambers TM, Kawaoka Y (1992) Evolution and ecology of influenza A viruses. Microbiol Rev 56: 152–179.
2. Rohm C, Zhou N, Suss J, Mackenzie J, Webster RG (1996) Characterization of a novel influenza hemagglutinin, H15: criteria for determination of influenza A subtypes. Virology 217: 508–516.
3. Fouchier RA, Munster V, Wallensten A, Bestebroer TM, Herfst S, et al. (2005) Characterization of a novel influenza A virus hemagglutinin subtype (H16) obtained from black-headed gulls. J Virol 79: 2814–2822.
4. Li KS, Guan Y, Wang J, Smith GJD, Xu KM, et al. (2004) Genesis of highly pathogenic and potentially pandemic H5N1 influenza virus in eastern Asia. Nature 430: 209–213.
5. Chen H, Smith G. J D, Zhang SY, Qin K, Wang J, Li KS, et al. (2005) H5N1 virus outbreak in migratory waterfowl. Nature 436: 191–192.
6. Ducatez MF, Olinger CM, Owoade AA, De Landtsheer, S Ammerlaan, W, et al. (2006) Avian flu: multiple introductions of H5N1 in Nigeria. Nature 442: 37.
7. Smith GJD, Fan XH, Wang J, Li KS, Qin K, et al. (2006) Emergence and predominance of an H5N1 influenza variant in China. Proc Natl Acad Sci USA 103: 16936–16941.
8. Wang G, Zhan D, Li L, Lei F, Liu B, et al. (2008) H5N1 avian influenza re-emergence of Lake Qinghai: phylogenetic and antigenic analyses of the newly isolated viruses and roles of migratory birds in virus circulation. J Gen Virol 89: 697–702.
9. Kajihara M, Matsuno K, Simulundu E, Muramatsu M, Noyori O, et al. (2011) An H5N1 highly pathogenic avian influenza virus that invaded Japan through waterfowl migration. Jpn J Vet Res 59: 89–100.
10. Sakoda Y, Ito H, Uchida Y, Okamatsu M, Yamamoto N, et al. (2012) Reintroduction of H5N1 highly pathogenic avian influenza virus by migratory water birds, causing poultry outbreaks in the 2010–2011 winter season in Japan. J Gen Virol 93: 541–550.
11. Gambotto A, Barratt-Boyes SM, de Jong MD, Neumann G, Kawaoka Y (2008) Human infection with highly pathogenic H5N1 influenza virus. Lancet 371: 1464–1475.
12. WHO. (2013) Cumulative number of confirmed human cases of avian influenza A(H5N1) reported to WHO. Available: http://www.who.int/influenza/human_animal_interface/H5N1_cumulative_table_archives/en/index.html. Accessed 14 May 2014.
13. Klenk HD, Garten W, Matrosovich M (2011) Molecular mechanisms of interspecies transmission and pathogenicity of influenza viruses: lessons from the 2009 pandemic. BioEssays 33: 180–188.
14. Both L, Banyard AC, van Dolleweerd C, Wright E, Ma JK, Fooks AR (2013) Monoclonal antibodies for prophylactic and therapeutic use against viral infections. Vaccine 31: 1553–1559.
15. Goudsmit J, Marissen WE, Weldon WC, Niezgoda M, Hanlon CA, et al. (2006) Comparison of an anti-rabies human monoclonal antibody combination with human polyclonal anti-rabies immune globulin. J Infect Dis 193: 796–801.
16. Müller T, Dietzschold B, Erdl H, Fooks AR, Freuling C, et al. (2009) Development of a mouse monoclonal antibody cocktail for post-exposure rabies prophylaxis in humans. PLoS Negl Trop Dis 3: e542.
17. Prosniak M, Faber M, Hanlon CA, Rupprecht CE, Hooper DC, Dietzschold B (2003) Development of a cocktail of recombinant-expressed human rabies virus-neutralizing monoclonal antibodies for postexposure prophylaxis of rabies. J Infect Dis 188: 53–56.
18. ter Meulen J, Bakker AB, van den Brink EN, Weverling GJ, Martina BE, et al. (2004) Human monoclonal antibody as prophylaxis for SARS coronavirus infection in ferrets. Lancet 363: 2139–2141.
19. ter Meulen J, van den Brink EN, Poon LL, Marissen WE, Leung CS, et al. (2006) Human monoclonal antibody combination against SARS coronavirus: synergy and coverage of escape mutants. PLoS Med 3: e237.
20. Bossart KN, Geisbert TW, Feldmann H, Zhu Z, Feldmann F, et al. (2011) A neutralizing human monoclonal antibody protects african green monkeys from hendra virus challenge. Sci Transl Med 3: 105ra103.
21. Bossart KN, Rockx B, Feldmann F, Brining D, Scott D, et al. (2012) A Hendra virus G glycoprotein subunit vaccine protects African green monkeys from Nipah virus challenge. Sci Transl Med 4: 146ra107.
22. Dye JM, Herbert AS, Kuehne AI, Barth JF, Muhammad MA, et al. (2012) Postexposure antibody prophylaxis protects nonhuman primates from filovirus disease. Proc Natl Acad Sci USA 109: 5034–5039.
23. Marzi A, Yoshida R, Miyamoto H, Ishijima M, Suzuki Y, et al. (2012) Protective efficacy of neutralizing monoclonal antibodies in a nonhuman primate model of Ebola hemorrhagic fever. PLoS One 7: e36192.
24. Qiu X, Audet J, Wong G, Pillet S, Bello A, et al. (2012) Successful treatment of ebola virus-infected cynomolgus macaques with monoclonal antibodies. Sci Transl Med 4: 138ra81.

25. Olinger GG Jr, Pettitt J, Kim D, Working C, Bohorov O, et al. (2012) Delayed treatment of Ebola virus infection with plant-derived monoclonal antibodies provides protection in rhesus macaques. Proc Natl Acad Sci USA 109: 18030–18035.
26. Kreijtz JH, Fouchier RA, Rimmelzwaan GF (2011) Immune responses to influenza virus infection. Virus Res 162: 19–30.
27. Le QM, Ito M, Muramoto Y, Hoang PV, Vuong CD, et al. (2010) Pathogenicity of highly pathogenic avian H5N1 influenza A viruses isolated from humans between 2003 and 2008 in northern Vietnam. J Gen Virol 91: 2485–2490.
28. Reed LJ, Muench H (1938) A simple method of estimating fifty percent endpoints. Am J Hyg 27: 493–497.
29. Pham VL, Nakayama M, Itoh Y, Ishigaki H, Kitano M, et al. (2013) Pathogenicity of pandemic H1N1 influenza A virus in immunocompromised cynomolgus macaques. PLoS One 8: e75910.
30. Kitano M, Itoh Y, Kodama M, Ishigaki H, Nakayama M, et al. (2011) Efficacy of single intravenous injection of peramivir against influenza B virus infection in ferrets and cynomolgus macaques. Antimicrob Agents Chemother 55: 4961–4970.
31. Daniels PS, Jeffries S, Yates P, Schild GC, Rogers GN, et al. (1987) The receptor-binding and membrane-fusion properties of influenza virus variants selected using anti-haemagglutinin monoclonal antibodies. EMBO J 6: 1459–1465.
32. Eisen MB, Sabesan S, Skehel JJ, Wiley DC (1997) Binding of the influenza A virus to cell-surface receptors: structures of five hemagglutinin-sialyloligosaccharide complexes determined by X-ray crystallography. Virology 232: 19–31.
33. Russell RJ, Stevens DJ, Haire LF, Gamblin SJ, Skehel JJ (2006) Avian and human receptor binding by hemagglutinins of influenza A viruses. Glycoconj J 23: 85–92.
34. Ha Y, Stevens DJ, Skehel JJ, Wiley DC (2001) X-ray structures of H5 avian and H9 swine influenza virus hemagglutinins bound to avian and human receptor analogs. Proc Natl Acad Sci USA 98: 11181–11186.
35. Hatta M, Gao P, Halfmann P, Kawaoka Y (2001) Molecular basis for high virulence of Hong Kong H5N1 influenza A viruses. Science 293: 1840–1842.
36. Park CH, Ishinaka M, Takada A, Kida H, Kimura T, et al. (2002) The invasion routes of neurovirulent A/Hong Kong/483/97 (H5N1) influenza virus into the central nervous system after respiratory infection in mice. Arch Virol 147: 1425–1436.
37. Nakayama M, Shichinohe S, Itoh Y, Ishigaki H, Kitano M, et al. (2013) Protection against H5N1 highly pathogenic avian and pandemic (H1N1) 2009 influenza virus infection in cynomolgus monkeys by an inactivated H5N1 whole particle vaccine. PLoS ONE 8: e82740.
38. Wu C, Lu X, Wang X, Jin T, Cheng X, et al. (2013) Clinical symptoms, immune factors, and molecular characteristics of an adult male in Shenzhen, China infected with influenza virus H5N1. J Med Virol 85: 760–768.
39. Nakajima N, Van Tin N, Sato Y, Thach HN, Katano H, et al. (2013) Pathological study of archival lung tissues from five fatal cases of avian H5N1 influenza in Vietnam. Mod Pathol 26: 357–369.
40. de Jong MD, Thanh TT, Khanh TH, Hien VM, Smith GJD, et al. (2005) Oseltamivir Resistance during Treatment of Influenza A (H5N1) Infection. N Engl J Med 353: 2667–2672.
41. Le QM, Kiso M, Someya K, Sakai YT, Nguyen TH, et al. (2005) Avian flu: Isolation of drug-resistant H5N1 virus. Nature 437: 1108–1108.
42. Boltz DA, Douangngeun B, Phommachanh P, Sinthasak S, Mondry R, et al. (2010) Emergence of H5N1 avian influenza viruses with reduced sensitivity to neuraminidase inhibitors and novel reassortants in Lao People's Democratic Republic. J Gen Virol 91(Pt 4): 949–959.
43. Zhou B, Zhong N, Guan Y (2007) Treatment with convalescent plasma for influenza A (H5N1) infection. N Engl J Med 357: 1450–1451.
44. Chen Y, Qin K, Wu WL, Li G, Zhang J, et al. (2009) Broad cross-protection against H5N1 avian influenza virus infection by means of monoclonal antibodies that map to conserved viral epitopes. J Infect Dis 199: 49–58.
45. Oh HL, Akerström S, Shen S, Bereczky S, Karlberg H, et al. (2010) An antibody against a novel and conserved epitope in the hemagglutinin 1 subunit neutralizes numerous H5N1 influenza viruses. J Virol 84: 8275–8286.
46. Corti D, Voss J, Gamblin SJ, Codoni G, Macagno A, et al. (2011) A neutralizing antibody selected from plasma cells that binds to group 1 and group 2 influenza A hemagglutinins. Science 333: 850–856.
47. Hanson BJ, Boon AC, Lim AP, Webb A, Ooi EE, et al. (2006) Passive immunoprophylaxis and therapy with humanized monoclonal antibody specific for influenza A H5 hemagglutinin in mice. Respir Res 7: 126.
48. Maneewatch S, Thanongsaksrikul J, Songserm T, Thueng-In K, Kulkeaw K, et al. (2009) Human single-chain antibodies that neutralize homologous and heterologous strains and clades of influenza A virus subtype H5N1. Antivir Ther 14: 221–230.
49. Sui J, Hwang WC, Perez S, Wei G, Aird D, et al. (2009) Structural and functional bases for broad-spectrum neutralization of avian and human influenza A viruses. Nat Struct Mol Biol 16: 265–273.
50. van den Brand JM, Haagmans BL, van Riel D, Osterhaus AD, Kuiken T. (2014) The Pathology and Pathogenesis of Experimental Severe Acute Respiratory Syndrome and Influenza in Animal Models. J Comp Pathol (in press).
51. Prabakaran M, Prabhu N, He F, Hongliang Q, Ho HT, et al. (2009) Combination therapy using chimeric monoclonal antibodies protects mice from lethal H5N1 infection and prevents formation of escape mutants. PLoS One 4: e5672.

Biochemical and Biophysical Research Communications 450 (2014) 942–947

Contents lists available at ScienceDirect

Biochemical and Biophysical Research Communications

journal homepage: www.elsevier.com/locate/ybbrc

Identification of SIV Nef CD8$^+$ T cell epitopes restricted by a MHC class I haplotype associated with lower viral loads in a macaque AIDS model

Takushi Nomura [a,*], Hiroyuki Yamamoto [a], Naofumi Takahashi [a], Taeko K. Naruse [b], Akinori Kimura [b], Tetsuro Matano [a,c,*]

[a] AIDS Research Center, National Institute of Infectious Diseases, 1-23-1 Toyama, Shinjuku-ku, Tokyo 162-8640, Japan
[b] Department of Molecular Pathogenesis, Medical Research Institute, Tokyo Medical and Dental University, 2-3-10 Kandasurugadai, Chiyoda-ku, Tokyo 101-0062, Japan
[c] The Institute of Medical Science, The University of Tokyo, 4-6-1 Shirokanedai, Minato-ku, Tokyo 108-8639, Japan

ARTICLE INFO

Article history:
Received 6 June 2014
Available online 24 June 2014

Keywords:
HIV
SIV
CD8$^+$ T cell
MHC-I
Epitope

ABSTRACT

Virus-specific CD8$^+$ T-cell responses are crucial for the control of human immunodeficiency virus (HIV) and simian immunodeficiency virus (SIV) replication. Multiple studies on HIV-infected individuals and SIV-infected macaques have indicated association of several major histocompatibility complex class I (MHC-I) genotypes with lower viral loads and delayed AIDS progression. Understanding of the viral control mechanism associated with these MHC-I genotypes would contribute to the development of intervention strategy for HIV control. We have previously reported a rhesus MHC-I haplotype, *90-120-Ia*, associated with lower viral loads after SIVmac239 infection. $Gag_{206-216}$ and $Gag_{241-249}$ epitope-specific CD8$^+$ T-cell responses have been shown to play a central role in the reduction of viral loads, whereas the effect of Nef-specific CD8$^+$ T-cell responses induced in all the *90-120-Ia*$^+$ macaques on SIV replication remains unknown. Here, we identified three CD8$^+$ T-cell epitopes, Nef_{9-19}, Nef_{89-97}, and $Nef_{193-203}$, associated with *90-120-Ia*. Nef_{9-19} and $Nef_{193-203}$ epitope-specific CD8$^+$ T-cell responses frequently selected for mutations resulting in viral escape from recognition by these CD8$^+$ T cells, indicating that these CD8$^+$ T cells exert strong suppressive pressure on SIV replication. Results would be useful for elucidation of the viral control mechanism associated with *90-120-Ia*.

1. Introduction

In human immunodeficiency virus (HIV) and simian immunodeficiency virus (SIV) infections, host immune responses fail to eradicate viruses and allow persistent infection, leading to AIDS progression. Unlike most acute virus infections, effective neutralizing antibody responses are not efficiently induced in early HIV/SIV infection [1]. Virus-specific CD8$^+$ T-cell responses play an important role in the control of HIV/SIV replication [2–6]. CD8$^+$ T cells recognize antigenic peptides bound to polymorphic major histocompatibility complex class I (MHC-I) molecules, whose genotypes affect CD8$^+$ T-cell responses [7,8]. Several MHC-I genotypes have been shown to be associated with lower viral loads and slower disease progression in HIV/SIV infections [9–14]. Understanding of the viral control mechanism associated with these protective MHC-I alleles would contribute to the development of intervention strategy for HIV control.

Recent vaccine trials in macaque AIDS models have shown a possibility of SIV control by effective CD8$^+$ T-cell responses [15–19]. It has been indicated that CD8$^+$ T cells targeting Gag are effective against HIV/SIV infection [20–23]. Furthermore, current studies have suggested that Nef- and Vif-specific CD8$^+$ T-cell responses can contribute to SIV control in macaque AIDS models [24,25].

We have previously reported a rhesus MHC-I haplotype, *90-120-Ia*, associated with lower viral loads after SIVmac239 challenge [14]. In that study, those Burmese rhesus macaques possessing *90-120-Ia* had lower set-point plasma viral loads (geometric mean at 1 year after SIV challenge: 1.5×10^4 copies/ml); two of them controlled viremia for more than 4 years while the remaining four developed AIDS in 4 years. Our vaccine trial has shown that all the *90-120-Ia*$^+$ macaques immunized with DNA-prime/Gag-expressing Sendai virus (SeV-Gag) vector-boost controlled a SIVmac239 challenge [26]. Mamu-A1*043:01-restricted $Gag_{206-216}$ (IINEEAADWDL) and Mamu-A1*065:01-restricted $Gag_{241-249}$ (SSVDEQIQW) epitope-specific CD8$^+$ T-cell responses were responsible for this viral control

* Corresponding authors. Address: AIDS Research Center, National Institute of Infectious Diseases, 1-23-1 Toyama, Shinjuku-ku, Tokyo 162-8640, Japan. Fax: +81 3 5285 1165.
E-mail addresses: nomutaku@nih.go.jp (T. Nomura), tmatano@nih.go.jp (T. Matano).

http://dx.doi.org/10.1016/j.bbrc.2014.06.072
0006-291X/

[26–28]. SIVmac239-infected *90-120-Ia*$^+$ macaques also elicited CD8$^+$ T-cell responses targeting Nef, which may be involved in viral control [14]. In the present study, we determined Nef CD8$^+$ T-cell epitopes associated with this MHC-I haplotype *90-120-Ia*.

2. Materials and methods

2.1. Samples

The present study used frozen plasma and peripheral mononuclear cell (PBMC) samples derived from ten Burmese rhesus macaques (*Macaca mulatta*) possessing MHC-I haplotype *90-120-Ia*. Our previous SIVmac239 challenge experiments using these animals [14,26–28] have been carried out in Tsukuba Primate Research Center in National Institute of Biomedical Innovation (NIBP) with the help of the Corporation for Production and Research of Laboratory Primates. These studies were approved by the Committee on the Ethics of Animal Experiments of NIBP under the guideline for animal experiments at NIBP and the National Institute of Infectious Diseases which is in accordance with the Guidelines for Proper Conduct of Animal Experiments established by the Science Council of Japan (http://www.scj.go.jp/ja/info/kohyo/pdf/kohyo-20-k16-2e.pdf).

Macaques R06-037, R07-004, and R07-009 were unvaccinated and intravenously challenged with SIVmac239 [14]. Macaques R03-018 and R07-007 received a DNA-prime/SeV-boost vaccine eliciting $Gag_{206-216}$- and $Gag_{241-249}$-specific CD8$^+$ T-cell responses, respectively, before SIVmac239 challenge as described before [27,28]. Macaques R06-035, R06-041, R05-004, R05-027, and R07-005 received a DNA-prime/SeV-Gag-boost as described before [26]. Macaques R06-035 and R06-041 were intravenously challenged with SIVmac239Gag216S244E, a SIVmac239 carrying two *gag* mutations, GagL216S and GagD244E, leading to a leucine (L)-to-serine (S) substitution at the 216th amino acid (aa) and an aspartic acid (D)-to-glutamic acid (E) substitution at the 244th aa in Gag, whereas macaques R05-004, R05-027, and R07-005 with SIVmac239Gag216S244E247L312V373T, a SIVmac239 carrying five *gag* mutations, GagL216S, GagD244E, GagI247L (isoleucine [I] to L at the 247th aa), GagA312V (alanine [A] to valine [V] at the 312th aa), and GagA373T (A to threonine [T] at the 373rd aa) [26].

The determination of macaque MHC-I haplotypes was based on the family study in combination with the reference strand-mediated conformation analysis of *Mamu-A* and *Mamu-B* genes and detection of major *Mamu-A* and *Mamu-B* alleles by cloning the reverse transcription (RT)-PCR products [14,29,30]. Confirmed MHC-I alleles consisting of the MHC-I haplotype *90-120-Ia* are *Mamu-A1*043:01* (GenBank accession number AB444869), *Mamu-A1*065:01* (AB444921), *Mamu-B*061:03* (AB430442), *Mamu-B*068:04* (AM902571), and *Mamu-B*089:01* (EF580172).

2.2. Sequencing analysis of plasma viral genomes

Viral RNAs were extracted using the High Pure Viral RNA kit (Roche Diagnostics) from plasma. Fragments of cDNAs encoding SIVmac239 Nef were amplified by nested RT-PCR from plasma RNAs and subjected to direct sequencing by using dye terminator chemistry and an automated DNA sequencer (Applied Biosystems) [33].

2.3. Analysis of SIV peptide-specific CD8$^+$ T-cell responses

SIV peptide-specific CD8$^+$ T-cell responses were measured by flow-cytometric analysis of interferon-γ (IFN-γ) induction [25]. PBMCs (2.5×10^6 cells) were cocultured for 6 h with autologous herpesvirus papio-immortalized B-lymphoblastoid cell lines (B-LCLs; 1.0×10^6 cells) pulsed with 1–5 μM or indicated concentrations of peptides designed for epitope mapping in 96-well V-bottom microwell plates. Intracellular IFN-γ staining was performed using a Cytofix Cytoperm kit (BD). Fluorescein isothiocyanate-conjugated anti-human CD4 (BD), peridinin chlorophyll protein (PerCP)-conjugated anti-human CD8 (BD), allophycocyanin Cy7 (APC-Cy7)-conjugated anti-human CD3 (BD), and phycoerythrin (PE)-conjugated anti-human IFN-γ antibodies (Biolegend) were used. Specific T-cell frequencies were calculated by subtracting nonspecific IFN-γ$^+$ T-cell frequencies from those after peptide-specific stimulation. Specific T-cell frequencies less than 100 cells per million PBMCs were considered negative.

3. Results and discussion

3.1. Identification of three Nef CD8$^+$ T-cell epitopes associated with MHC-I haplotype 90–120-Ia

In our previous study [14], we examined viral genome sequences 1 year after SIVmac239 challenge in four groups of Burmese rhesus macaques possessing MHC-I haplotypes *90-120-Ia*, *90-120-Ib*, *90-010-Ie*, and *90-088-Ij*, respectively. Then, in the present study, we compared *nef* sequences in the four macaques possessing *90-120-Ia* with those in the remaining three groups ($n = 14$). Amino acid sequences revealed three regions in Nef, Nef12 (the 12th aa), Nef89/90 (the 89th or 90th aa), and Nef201/202 (the 201st or 202nd aa), which had substitutions in all *90-120-Ia*$^+$ animals but mostly not in others. Indeed, substitutions at Nef12 were observed only in two of the fourteen *90-120-Ia*-negative animals while substitutions at Nef89/90 or Nef201/202 were detected in none of them.

We tried to map CD8$^+$ T-cell epitopes around the regions described above to examine whether these *90-120-Ia*-associated *nef* mutations resulting in the Nef12, Nef89/90, and Nef201/202 amino acid substitutions were selected by CD8$^+$ T cells. Analysis using available samples derived from ten *90-120-Ia*$^+$ macaques identified three CD8$^+$ T-cell epitopes, Nef_{9-19} (RSRPSGDLRQR), Nef_{89-97} (DIDEEDDDL), and $Nef_{193-203}$ (YLMHPAQTSQW) (Fig. 1A). The endpoint peptide concentrations for CD8$^+$ T-cell responses were 10–100 nM against Nef_{9-19} epitope and 1–10 nM against $Nef_{193-203}$ (Fig. 1B). The endpoint was very low, less than 0.1 nM, for Nef_{89-97} epitope (Fig. 1B), indicating extremely high binding affinity of this epitope.

3.2. Determination of MHC-I alleles restricting CD8$^+$ T-cell epitopes

Nef_{9-19} epitope-specific CD8$^+$ T-cell responses in the early phase of SIV infection were examined in six *90-120-Ia*$^+$ animals, all of which showed positive responses (Fig. 2A), indicating that this epitope is associated with MHC-I haplotype *90-120-Ia*. On the other hand, Nef_{89-97} and $Nef_{193-203}$ epitope-specific CD8$^+$ T-cell responses in the early phase were detected not in all but in three of the seven and two of the four examined *90-120-Ia*$^+$ animals, respectively (Fig. 2A).

We then tried to determine *90-120-Ia*-derived MHC-I alleles restricting these CD8$^+$ T-cell epitopes. HLA-A/B/C-negative human 721.221 cell lines expressing *Mamu-A1*043:01*, *Mamu-A1*065:01*, and *Mamu-B*061:03* were available for the analysis. Nef_{89-97}-specific CD8$^+$ T-cell responses were detected on *Mamu-A1*043:01*-expressing 721.221 cells, whereas $Nef_{193-203}$-specific CD8$^+$ T-cell responses were detected on *Mamu-A1*065:01*-expressing 721.221 cells (Fig. 2B). These results indicate that the Nef_{89-97} and $Nef_{193-203}$ epitopes are restricted by Mamu-A1*043:01 and Mamu-A1*065:01, respectively. However, Nef_{9-19} epitope-specific CD8$^+$ T-cell responses were not detected on any of 721.221 cells expressing *Mamu-A1*043:01*, *Mamu-A1*065:01*, or *Mamu-B*061:03*,

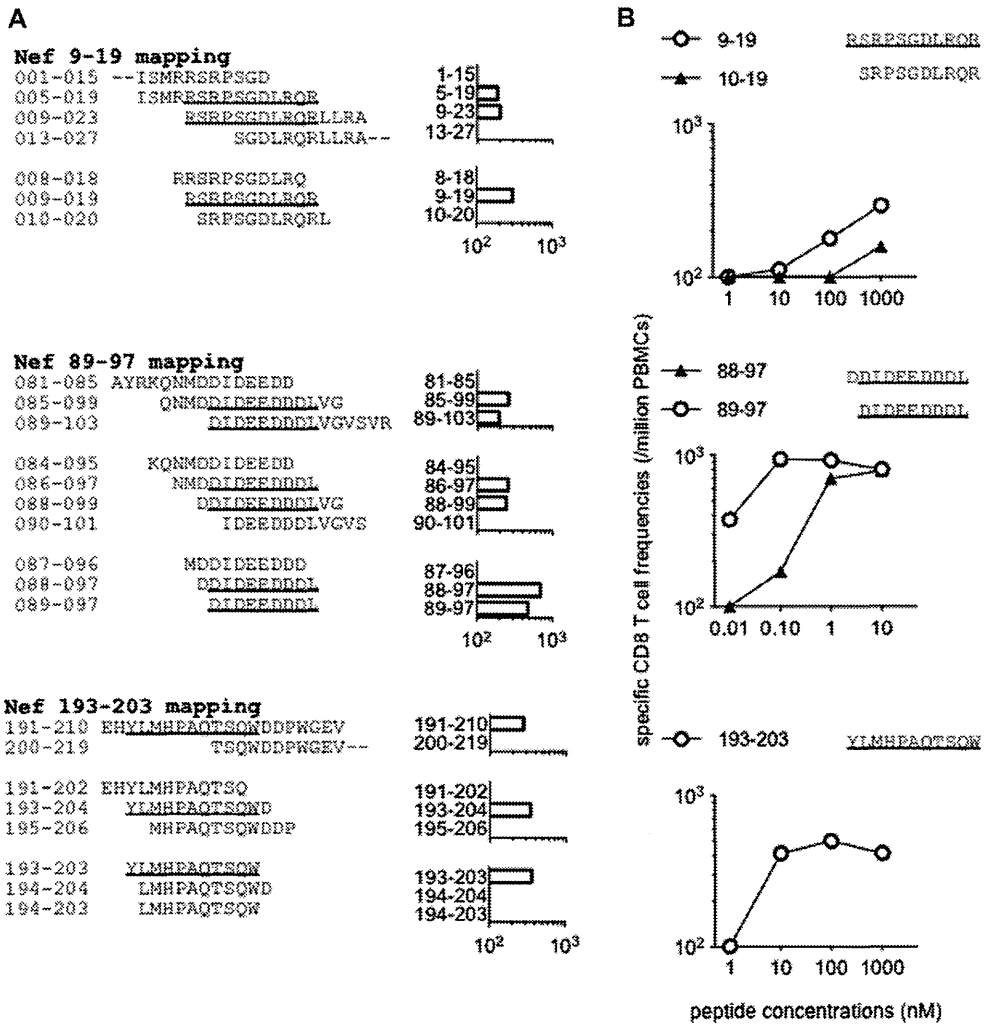

Fig. 1. Mapping of CD8$^+$ T-cell epitopes, Nef_{9-19}, Nef_{89-97}, and $Nef_{193-203}$. (A) Summarized data for mapping of Nef_{9-19} (top panels), Nef_{89-97} (middle), and $Nef_{193-203}$ (bottom) epitopes using PBMCs of SIV-infected *90-120-Ia*$^+$ animals. CD8$^+$ T-cell frequencies specific for the indicated peptides are shown (/million PBMCs). Representative results using PBMCs from R05-027 and R06-041 (top), R03-018 (middle), and R07-004 and R07-007 (bottom) are shown. (B) CD8$^+$ T-cell responses under the indicated concentrations of Nef_{9-19} and Nef_{10-19} (top panel), Nef_{88-97} and Nef_{89-97} (middle), and $Nef_{193-203}$ (bottom) peptides. Representative results using PBMCs from R05-004 (top), R03-018 (middle), and R07-009 (bottom) are shown.

implying that this epitope is restricted by a *90-120-Ia*-derived MHC-I molecule other than the above three (Fig. 2B).

3.3. Mutations resulting in viral escape from CD8$^+$ T-cell recognition

In our previous study [14], SIV-infected *90-120-Ia*$^+$ macaques had mutations resulting in Nef12, Nef89/90, and Nef201/202 amino acid substitutions as described above. The substituted amino acids were different at Nef89/90 in individual four animals, but three of the four had the same substitutions at Nef12 and Nef201, NefP12Q (proline [P]-to-glutamine [Q]) and NefS201Y (S-to-tyrosine [Y]), respectively. We examined whether these two *90-120-Ia*-associated *nef* mutations result in viral escape from CD8$^+$ T-cell responses specific for the epitopes we identified. Nef_{9-19} peptide-specific CD8$^+$ T-cell responses were reduced by the NefP12Q substitution (Fig. 3A). Also, the NefP12T substitution (a P-to-T substitution at the 12th aa in Nef) that was observed in the remaining one SIV-infected *90-120-Ia*$^+$ macaque resulted in viral escape from Nef_{9-19}-specific CD8$^+$ T-cell responses. $Nef_{193-203}$ peptide-specific CD8$^+$ T-cell responses were reduced by the NefS201Y (Fig. 3A). Selection of these escape mutations in SIV infection implies that these Nef_{9-19} and $Nef_{193-203}$ epitope-specific CD8$^+$ T cells exert suppressive pressure on SIV replication. The latter $Nef_{193-203}$ epitope overlaps with previously-reported MW9 ($Nef_{195-203}$) and HW8 ($Nef_{196-203}$) epitopes [32,33]. The MW9 is restricted by Mamu-B*17 [12], a protective MHC-I against SIVmac239 infection, while the HW8 is restricted by a MHC-I in a group of Mauritian cynomolgus macaques that frequently control SIVmac239 replication. Thus, this $Nef_{193-203}$ region may be a promising CD8$^+$ T-cell target for SIV control.

Further analysis of viral *nef* nucleotide sequences found relatively rapid selection of a mutation encoding Nef12, NefP12Q, NefP12S, or NefS13P, in two months after SIV infection in macaques R05-004, R05-027, R06-035, R06-041, and R07-005 (Fig. 3B). The NefP12S and NefS13P substitutions also resulted in viral escape from Nef_{9-19}-specific CD8$^+$ T-cell responses (Fig. 3A). However, no mutation was selected in the region encoding Nef_{89-97} or $Nef_{193-203}$ epitope in two months (Fig. 3B). In the early phase, Nef_{9-19}-specific CD8$^+$ T-cell responses were induced in all whereas Nef_{89-97}- and $Nef_{193-203}$-specific CD8$^+$ T-cell responses were detectable only in some of them, as described above. These results suggest that *90-120-Ia*$^+$ macaques predominantly elicit Nef_{9-19}-specific CD8$^+$ T-cell responses resulting in selection of Nef12/13 mutations in the early phase of SIV infection, followed by induction of Nef_{89-97}- and $Nef_{193-203}$-specific CD8$^+$ T-cell responses resulting in selection of Nef89/90 and Nef201/202 mutations in the chronic phase.

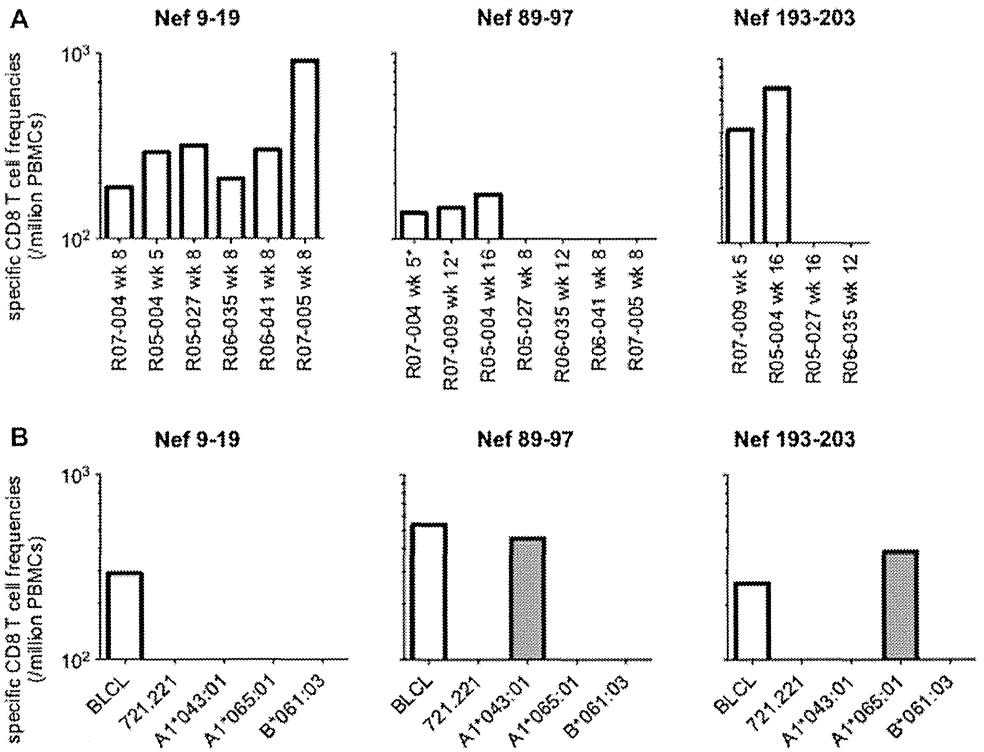

Fig. 2. Nef_{9-19}, Nef_{89-97}, and $Nef_{193-203}$ epitope-specific $CD8^+$ T-cell responses. (A) $CD8^+$ T-cell responses specific for Nef_{9-19} (left panel), Nef_{89-97} (middle), and $Nef_{193-203}$ (right) epitopes in the early phase of SIV infection in *90-120-Ia*$^+$ macaques. The asterisk indicates $CD8^+$ T-cell responses specific for Nef_{86-97} peptide. (B) Nef_{9-19}- (left panel), Nef_{89-97}- (middle), and $Nef_{193-203}$-specific (right) $CD8^+$ T-cell responses after coculture with peptide-pulsed B-LCLs, 721.221 cells, or 721.221 cells expressing *Mamu-A1*043:01*, *Mamu-A1*065:01*, or *Mamu-B*061:03*. These cells were pulsed with 1,000 nM Nef_{9-19} peptides (left), 1 nM Nef_{89-97} peptides (middle), and 100 nM $Nef_{193-203}$ peptides (right), respectively. Representative results using PBMCs from R06-035 for Nef_{9-19}, R03-018 for Nef_{89-97}, and R07-004 for $Nef_{193-203}$ are shown.

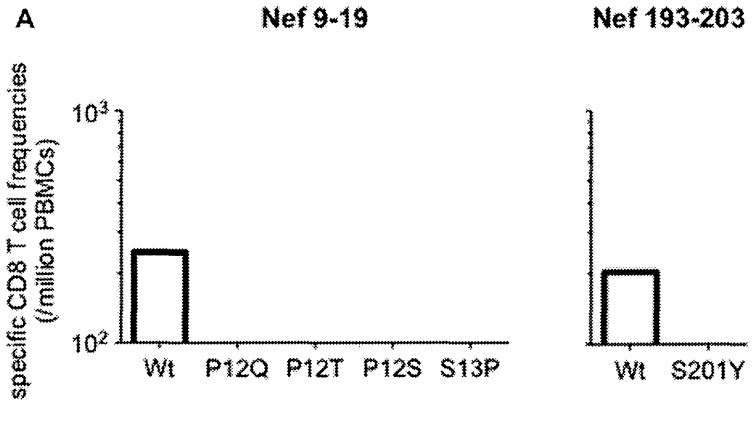

Fig. 3. $CD8^+$ T-cell escape mutations. (A) $CD8^+$ T-cell responses specific for the wild-type or mutant Nef_{9-19} peptides with the indicated substitutions (left panel) or the wild-type or a mutant $Nef_{193-203}$ peptide with S201Y substitution (right). Representative results using PBMCs from R07-005 for Nef_{9-19} and R07-004 for $Nef_{193-203}$ are shown. (B) Predominant nonsynonymous mutations in plasma viral *nef* regions encoding Nef_{9-19}, Nef_{89-97}, and $Nef_{193-203}$ epitopes in 3 months after SIV challenge in *90-120-Ia*$^+$ macaques. Amino acid substitutions are shown.

Our previous study [14] frequently found $CD8^+$ T-cell responses targeting Vif and a viral genome mutation resulting in VifP115S substitution (a P-to-S substitution at the 115th aa in Vif) in SIV-infected *90-120-Ia*$^+$ macaques. Then, in the present study, we identified a $CD8^+$ T-cell epitope, $Vif_{114-124}$ (FPCFTAGEVRR). The endpoint peptide concentration for $Vif_{114-124}$-specific $CD8^+$ T-cell

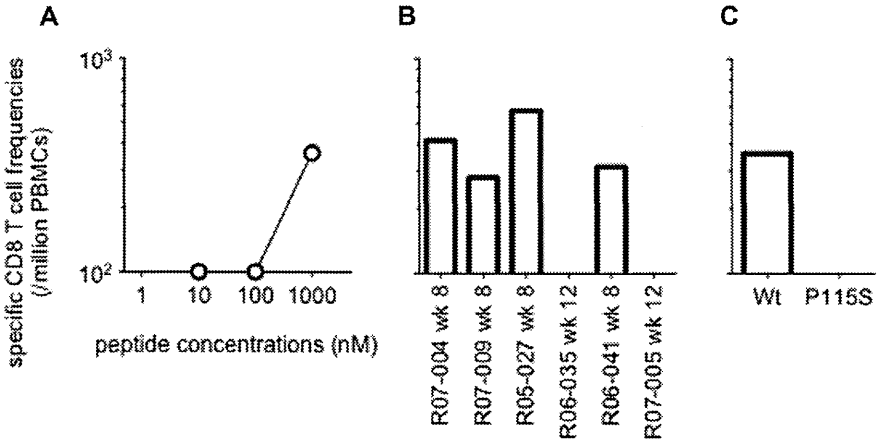

Fig. 4. Characterization of $Vif_{114-124}$ epitope-specific $CD8^+$ T-cell responses. (A) $CD8^+$ T-cell responses under the indicated concentrations of $Vif_{114-124}$ peptides. A representative result using PBMCs from R07-004 is shown. (B) $Vif_{114-124}$-specific $CD8^+$ T-cell responses in the early phase of SIV infection in *90-120-Ia*$^+$ macaques. (C) $CD8^+$ T-cell responses specific for the wild-type or a mutant $Vif_{114-124}$ peptide with P115S substitution. A representative result using PBMCs from R07-004 is shown.

responses was very high, more than 100 nM, indicating lower binding affinity of this epitope (Fig. 4A). $Vif_{114-124}$ epitope-specific $CD8^+$ T-cell responses were detected in the early phase in four of the six examined *90-120-Ia*$^+$ animals (Fig. 4B). The VifP115S substitution resulted in diminishment of $Vif_{114-124}$ peptide-specific $CD8^+$ T-cell responses, suggesting selective pressure by $CD8^+$ T cells targeting this epitope (Fig. 4C).

In summary, we identified three *90-120-Ia*-associated Nef $CD8^+$ T-cell epitopes, Nef_{9-19}, Nef_{89-97}, and $Nef_{193-203}$, in addition to the three previously-identified Gag epitopes, $Gag_{206-216}$, $Gag_{241-249}$, and $Gag_{373-380}$ [31]. Additionally, we identified a Vif $CD8^+$ T-cell epitope, $Vif_{114-124}$. In our previous study [26], all the *90-120-Ia*$^+$ macaques vaccinated with DNA-prime/SeV-Gag-boost controlled SIVmac239 replication without detectable viral loads after week 5 post-challenge, whereas those vaccinated animals (R05-004, R05-027, R06-035, R06-041, and R07-005) failed to show such rapid control of a challenge with SIVs carrying $Gag_{206-216}$-, $Gag_{241-249}$-, and $Gag_{373-380}$-specific $CD8^+$ T-cell escape mutations. This indicates that these $Gag_{206-216}$, $Gag_{241-249}$, and $Gag_{373-380}$ epitope-specific $CD8^+$ T-cell responses are responsible for the rapid SIVmac239 control. Macaques R05-004 and R05-027 showed persistent viremia and developed AIDS, whereas the remaining three (R06-035, R06-041, and R07-005) exhibited lower viral loads. The present study suggests involvement of Nef epitope-specific $CD8^+$ T-cell responses in this suppression of SIV replication in *90-120-Ia*$^+$ macaques.

Acknowledgments

This work was supported by a Grant-in-Aid for Scientific Research on Innovative Areas (#25115520) from the Ministry of Education, Culture, Sports, Science, and Technology in Japan and grants-in-aid from the Ministry of Health, Labor, and Welfare in Japan.

References

[1] D.R. Burton, R.C. Desrosiers, R.W. Doms, W.C. Koff, P.D. Kwong, J.P. Moore, G.J. Nabel, J. Sodroski, I.A. Wilson, R.T. Wyatt, HIV vaccine design and the neutralizing antibody problem, Nat. Immunol. 5 (2004) 233–236.
[2] R.A. Koup, J.T. Safrit, Y. Cao, C.A. Andrews, G. McLeod, W. Borkowsky, C. Farthing, D.D. Ho, Temporal association of cellular immune responses with the initial control of viremia in primary human immunodeficiency virus type 1 syndrome, J. Virol. 68 (1994) 4650–4655.
[3] P. Borrow, H. Lewicki, B.H. Hahn, G.M. Shaw, M.B. Oldstone, Virus-specific $CD8^+$ cytotoxic T-lymphocyte activity associated with control of viremia in primary human immunodeficiency virus type 1 infection, J. Virol. 68 (1994) 6103–6110.
[4] T. Matano, R. Shibata, C. Siemon, M. Connors, H.C. Lane, M.A. Martin, Administration of an anti-CD8 monoclonal antibody interferes with the clearance of chimeric simian/human immunodeficiency virus during primary infections of rhesus macaques, J. Virol. 72 (1998) 164–169.
[5] X. Jin, D.E. Bauer, S.E. Tuttleton, S. Lewin, A. Gettie, J. Blanchard, C.E. Irwin, J.T. Safrit, J. Mittler, L. Weinberger, L.G. Kostrikis, L. Zhang, A.S. Perelson, D.D. Ho, Dramatic rise in plasma viremia after CD8(+) T cell depletion in simian immunodeficiency virus-infected macaques, J. Exp. Med. 189 (1999) 991–998.
[6] J.E. Schmitz, M.J. Kuroda, S. Santra, V.G. Sasseville, M.A. Simon, M.A. Lifton, P. Racz, K. Tenner-Racz, M. Dalesandro, B.J. Scallon, J. Ghrayeb, M.A. Forman, D.C. Montefiori, E.P. Rieber, N.L. Letvin, K.A. Reimann, Control of viremia in simian immunodeficiency virus infection by CD8+ lymphocytes, Science 283 (1999) 857–860.
[7] P.J. Goulder, D.I. Watkins, Impact of MHC class I diversity on immune control of immunodeficiency virus replication, Nat. Rev. Immunol. 8 (2008) 619–630.
[8] T. Nomura, T. Matano, Association of MHC-I genotypes with disease progression in HIV/SIV infections, Front. Microbiol. 3 (2012) 234.
[9] S.A. Migueles, M.S. Sabbaghian, W.L. Shupert, M.P. Bettinotti, F.M. Marincola, L. Martino, C.W. Hallahan, S.M. Selig, D. Schwartz, J. Sullivan, M. Connors, HLA B*5701 is highly associated with restriction of virus replication in a subgroup of HIV-infected long term nonprogressors, Proc. Natl. Acad. Sci. U.S.A. 97 (2000) 2709–2714.
[10] T. Muhl, M. Krawczak, P. Ten Haaft, G. Hunsmann, U. Sauermann, MHC class I alleles influence set-point viral load and survival time in simian immunodeficiency virus-infected rhesus monkeys, J. Immunol. 169 (2002) 3438–3446.
[11] M. Altfeld, E.T. Kalife, Y. Qi, H. Streeck, M. Lichterfeld, M.N. Johnston, N. Burgett, M.E. Swartz, A. Yang, G. Alter, X.G. Yu, A. Meier, J.K. Rockstroh, T.M. Allen, H. Jessen, E.S. Rosenberg, M. Carrington, B.D. Walker, HLA alleles associated with delayed progression to AIDS contribute strongly to the initial CD8(+) T cell response against HIV-1, PLoS Med. 3 (2006) e403.
[12] L.J. Yant, T.C. Friedrich, R.C. Johnson, G.E. May, N.J. Maness, A.M. Enz, J.D. Lifson, D.H. O'Connor, M. Carrington, D.I. Watkins, The high-frequency major histocompatibility complex class I allele Mamu-B*17 is associated with control of simian immunodeficiency virus SIVmac239 replication, J. Virol. 80 (2006) 5074–5077.
[13] J.T. Loffredo, J. Maxwell, Y. Qi, C.E. Glidden, G.J. Borchardt, T. Soma, A.T. Bean, D.R. Beal, N.A. Wilson, W.M. Rehrauer, J.D. Lifson, M. Carrington, D.I. Watkins, Mamu-B*08-positive macaques control simian immunodeficiency virus replication, J. Virol. 81 (2007) 8827–8832.
[14] T. Nomura, H. Yamamoto, T. Shiino, N. Takahashi, T. Nakane, N. Iwamoto, H. Ishii, T. Tsukamoto, M. Kawada, S. Matsuoka, A. Takeda, K. Terahara, Y. Tsunetsugu-Yokota, N. Iwata-Yoshikawa, H. Hasegawa, T. Sata, T.K. Naruse, A. Kimura, T. Matano, Association of major histocompatibility complex class I haplotypes with disease progression after simian immunodeficiency virus challenge in Burmese rhesus macaques, J. Virol. 86 (2012) 6481–6490.
[15] T. Matano, M. Kobayashi, H. Igarashi, A. Takeda, H. Nakamura, M. Kano, C. Sugimoto, K. Mori, A. Iida, T. Hirata, M. Hasegawa, T. Yuasa, M. Miyazawa, Y. Takahashi, M. Yasunami, A. Kimura, D.H. O'Connor, D.I. Watkins, Y. Nagai, Cytotoxic T lymphocyte-based control of simian immunodeficiency virus replication in a preclinical AIDS vaccine trial, J. Exp. Med. 199 (2004) 1709–1718.
[16] N.L. Letvin, J.R. Mascola, Y. Sun, D.A. Gorgone, A.P. Buzby, L. Xu, Z.Y. Yang, B. Chakrabarti, S.S. Rao, J.E. Schmitz, D.C. Montefiori, B.R. Barker, F.L. Bookstein, G.J. Nabel, Preserved CD4+ central memory T cells and survival in vaccinated SIV-challenged monkeys, Science 312 (2006) 1530–1533.

[17] N.A. Wilson, J. Reed, G.S. Napoe, S. Piaskowski, A. Szymanski, J. Furlott, E.J. Gonzalez, L.J. Yant, N.J. Maness, G.E. May, T. Soma, M.R. Reynolds, E. Rakasz, R. Rudersdorf, A.B. McDermott, D.H. O'Connor, T.C. Friedrich, D.B. Allison, A. Patki, L.J. Picker, D.R. Burton, J. Lin, L. Huang, D. Patel, G. Heindecker, J. Fan, M. Citron, M. Horton, F. Wang, X. Liang, J.W. Shiver, D.R. Casimiro, D.I. Watkins, Vaccine-induced cellular immune responses reduce plasma viral concentrations after repeated low-dose challenge with pathogenic simian immunodeficiency virus SIVmac239, J. Virol. 80 (2006) 5875–5885.

[18] J. Liu, K.L. O'Brien, D.M. Lynch, N.L. Simmons, A. La Porte, A.M. Riggs, P. Abbink, R.T. Coffey, L.E. Grandpre, M.S. Seaman, G. Landucci, D.N. Forthal, D.C. Montefiori, A. Carville, K.G. Mansfield, M.J. Havenga, M.G. Pau, J. Goudsmit, D.H. Barouch, Immune control of an SIV challenge by a T-cell-based vaccine in rhesus monkeys, Nature 457 (2009) 87–91.

[19] S.G. Hansen, J.C. Ford, M.S. Lewis, A.B. Ventura, C.M. Hughes, L. Coyne-Johnson, N. Whizin, K. Oswald, R. Shoemaker, T. Swanson, A.W. Legasse, M.J. Chiuchiolo, C.L. Parks, M.K. Axthelm, J.A. Nelson, M.A. Jarvis, M. Piatak Jr., J.D. Lifson, L.J. Picker, Profound early control of highly pathogenic SIV by an effector memory T-cell vaccine, Nature 473 (2011) 523–527.

[20] B.H. Edwards, A. Bansal, S. Sabbaj, J. Bakari, M.J. Mulligan, P.A. Goepfert, Magnitude of functional CD8+ T-cell responses to the gag protein of human immunodeficiency virus type 1 correlates inversely with viral load in plasma, J. Virol. 76 (2002) 2298–2305.

[21] R. Zuniga, A. Lucchetti, P. Galvan, S. Sanchez, C. Sanchez, A. Hernandez, H. Sanchez, N. Frahm, C.H. Linde, H.S. Hewitt, W. Hildebrand, M. Altfeld, T.M. Allen, B.D. Walker, B.T. Korber, T. Leitner, J. Sanchez, C. Brander, Relative dominance of Gag p24-specific cytotoxic T lymphocytes is associated with human immunodeficiency virus control, J. Virol. 80 (2006) 3122–3125.

[22] P. Kiepiela, K. Ngumbela, C. Thobakgale, D. Ramduth, I. Honeyborne, E. Moodley, S. Reddy, C. de Pierres, Z. Mncube, N. Mkhwanazi, K. Bishop, M. van der Stok, K. Nair, N. Khan, H. Crawford, R. Payne, A. Leslie, J. Prado, A. Prendergast, J. Frater, N. McCarthy, C. Brander, G.H. Learn, D. Nickle, C. Rousseau, H. Coovadia, J.I. Mullins, D. Heckerman, B.D. Walker, P. Goulder, CD8+ T-cell responses to different HIV proteins have discordant associations with viral load, Nat. Med. 13 (2007) 46–53.

[23] J.A. Borghans, A. Molgaard, R.J. de Boer, C. Kesmir, HLA alleles associated with slow progression to AIDS truly prefer to present HIV-1 p24, PLoS One 2 (2007) e920.

[24] P.A. Mudd, M.A. Martins, A.J. Ericsen, D.C. Tully, K.A. Power, A.T. Bean, S.M. Piaskowski, L. Duan, A. Seese, A.D. Gladden, K.L. Weisgrau, J.R. Furlott, Y.I. Kim, M.G. Veloso de Santana, E. Rakasz, S. Capuano 3rd, N.A. Wilson, M.C. Bonaldo, R. Galler, D.B. Allison, M. Piatak Jr., A.T. Haase, J.D. Lifson, T.M. Allen, D.I. Watkins, Vaccine-induced CD8+ T cells control AIDS virus replication, Nature 491 (2012) 129–133.

[25] N. Iwamoto, N. Takahashi, S. Seki, T. Nomura, H. Yamamoto, M. Inoue, T. Shu, T.K. Naruse, A. Kimura, T. Matano, Control of simian immunodeficiency virus replication by vaccine-induced Gag- and Vif-specific CD8+ T cells, J. Virol. 88 (2014) 425–433.

[26] M. Kawada, T. Tsukamoto, H. Yamamoto, N. Iwamoto, K. Kuribara, A. Takeda, C. Moriya, H. Takeuchi, H. Akari, T. Matano, Gag-specific cytotoxic T-lymphocyte-based control of primary simian immunodeficiency virus replication in a vaccine trial, J. Virol. 82 (2008) 10199–10206.

[27] T. Tsukamoto, A. Takeda, T. Yamamoto, H. Yamamoto, M. Kawada, T. Matano, Impact of cytotoxic-T-lymphocyte memory induction without virus-specific CD4+ T-Cell help on control of a simian immunodeficiency virus challenge in rhesus macaques, J. Virol. 83 (2009) 9339–9346.

[28] H. Ishii, M. Kawada, T. Tsukamoto, H. Yamamoto, S. Matsuoka, T. Shiino, A. Takeda, M. Inoue, A. Iida, H. Hara, T. Shu, M. Hasegawa, T.K. Naruse, A. Kimura, M. Takiguchi, T. Matano, Impact of vaccination on cytotoxic T lymphocyte immunodominance and cooperation against simian immunodeficiency virus replication in rhesus macaques, J. Virol. 86 (2012) 738–745.

[29] J.R. Arguello, A.M. Little, A.L. Pay, D. Gallardo, I. Rojas, S.G. Marsh, J.M. Goldman, J.A. Madrigal, Mutation detection and typing of polymorphic loci through double-strand conformation analysis, Nat. Genet. 18 (1998) 192–194.

[30] T.K. Naruse, Z. Chen, R. Yanagida, T. Yamashita, Y. Saito, K. Mori, H. Akari, Y. Yasutomi, M. Miyazawa, T. Matano, A. Kimura, Diversity of MHC class I genes in Burmese-origin rhesus macaques, Immunogenetics 62 (2010) 601–611.

[31] M. Kawada, H. Igarashi, A. Takeda, T. Tsukamoto, H. Yamamoto, S. Dohki, M. Takiguchi, T. Matano, Involvement of multiple epitope-specific cytotoxic T-lymphocyte responses in vaccine-based control of simian immunodeficiency virus replication in rhesus macaques, J. Virol. 80 (2006) 1949–1958.

[32] B.R. Mothe, J. Sidney, J.L. Dzuris, M.E. Liebl, S. Fuenger, D.I. Watkins, A. Sette, Characterization of the peptide-binding specificity of Mamu-B*17 and identification of Mamu-B*17-restricted epitopes derived from simian immunodeficiency virus proteins, J. Immunol. 169 (2002) 210–219.

[33] M.L. Budde, J.M. Greene, E.N. Chin, A.J. Ericsen, M. Scarlotta, B.T. Cain, N.H. Pham, E.A. Becker, M. Harris, J.T. Weinfurter, S.L. O'Connor, M. Piatak Jr., J.D. Lifson, E. Gostick, D.A. Price, T.C. Friedrich, D.H. O'Connor, Specific CD8+ T cell responses correlate with control of simian immunodeficiency virus replication in Mauritian cynomolgus macaques, J. Virol. 86 (2012) 7596–7604.

International Journal of
Immunology and Immunotherapy

Original Research : Open Access

Development of a Method for Detection of Shigatoxin-Producing *Escherichia coli* Belonging to Clinically Important Twelve O Serotypes Based on the Combination of PickPen-Assisted Immunomagnetic Separation and Loop-Mediated Isothermal Amplification

Ahmad Yaman Kayali[1], Oscar Escalante-Maldonado[1], Varaporn Vuddhakul[2], Kazuko Seto[3], Yoshitsugu Nakaguchi[4], and Mitsuaki Nishibuchi[1,4]*

[1]*Graduate School of Medicine, Kyoto University, Japan*

[2]*Prince of Songkla University, Hat Yai, Thailand*

[3]*Osaka Prefectural Institute of Public Health, Osaka, Japan*

[4]*Centre for Southeast Asian Studies, Kyoto University, Japan*

***Corresponding author:** *Mitsuaki Nishibuchi, Center for Southeast Asian Studies, Kyoto University, 46 Shimoadachi-cho, Yoshida, Sakyo-ku, Kyoto 606-8501, Japan, Tel: +81-75-753-7367, Fax: +81-75-753-7319, E-mail: nisibuti@cseas.kyoto-u.ac.jp*

Abstract

Not only O157 Shigatoxin-producing *Escherichia coli* (STEC) but some of non-O157 STECs are attracting attentions as clinically important STEC and a possible food-borne spread of these pathogens is becoming a worldwide concern. In this study, we developed a sensitive, specific, and simple method to detect STECs of clinical significance in retail beef so that it can be used even in resource-limited countries. We designed and fine-tuned a protocol characterized by PickPen device-assisted immunomagnetic separation (IMS) for specific and simultaneous screening of O157 and eleven other O serotypes and quick and easy *stx* gene detection in STEC by the loop-mediated isothermal amplification (LAMP) assay. In vitro experiments showed 91CFU/ml sensitivity for IMS and 100% specificity for the IMS-LAMP-based method. We detected by the IMS-LAMP-based method the *stx* gene in 41 of 74 (55.4%) and none of 28 (0%) of beef purchased in, respectively, Thailand and Japan. Analyses of the STEC isolates from the Thai beef demonstrated high sensitivity and high (80-100 %) specificity of the detection method and regional difference in the STEC distribution in beef; and therefore the results support that this IMS-LAMP-based method is suitable for detection of clinically important STEC in beef.

Keywords

Shigatoxin-producing *Escherichia coli*, Retail beef, Immunomagnetic separation, PickPen, loop-mediated isothermal amplification

List of abbreviations

STEC: Shigatoxin-Producing *Escherichia coli*, EHEC: Enterohaemorrhagic *Escherichia coli*, *stx*: Shigatoxin gene, stx_1: Shigatoxin gene type 1, stx_2: Shigatoxin gene type 2, IMS: Immunomagnetic Separation, IMB: Immunomagnetic Beads, IMBv: Immunomagnetic Beads Volume, bIMBv: Best Immunomagnetic Beads Volume, LAMP: Loop-Mediated Isothermal Amplification, CE: Capture Efficiency

Introduction

Shiga toxin (Stx)-producing *Escherichia coli* (STEC; also called verocytotoxin-producing *E. coli* or VTEC) can cause mild diarrhea in humans. Enterohaemorrhagic *E. coli* (EHEC) is a highly virulent subgroup of STEC and is one of major categories of pathogenic *E. coli* that cause important enteric infections in humans [1]. The common virulence factor of STEC and EHEC is the production of one or both subtypes of Stx (Stx1 or Stx2). EHEC is defined, based on the typical symptom of the patient, as STEC causing severe bloody diarrhea in humans. The EHEC may be confirmed experimentally by detection of additional virulence factors intimin and the large EHEC plasmid [2].

Strains of STEC/EHEC are differentiated by the O antigen on their outer membrane into over 180 serotypes [3]. Of all EHEC serotypes *E. coli* O157:H7 is the one which has caused most food borne outbreaks and has led to the highest number of hemolytic uremic syndrome cases, a life-threatening sequela of STEC infection; however, some of non-O157 serotypes are also becoming an important health concern because they have been isolated from the patients with the typical symptoms of EHEC infection with increasing frequency than before [4,5]. EHEC belonging to O157 and six other O serotypes (O26, O91, O103, O111, O121, and O145) are considered important in Japan [6-8]; and additional eight serotypes (O15, O45, O55, O104, O113, O118, O128, and O153) totaling to fifteen O serotypes for all countries in the world [9-15]. We therefore considered these fifteen O serotypes of EHEC are of particular importance for a global-scale detection method.

ClinMed International Library

Citation: Kayali AY, Escalante-Maldonado O, Vuddhakul V, Seto K, Nakaguchi Y et al., (2015) Development of a Method for Detection of Shigatoxin-Producing Escherichia coli Belonging to Clinically Important Twelve O Serotypes Based on the Combination of PickPen-Assisted Immunomagnetic Separation and Loop-Mediated Isothermal Amplification. Int J Immunol Immunother. 2:004

Received: January 10, 2015: **Accepted:** January 20, 2015: **Published:** January 22, 2015

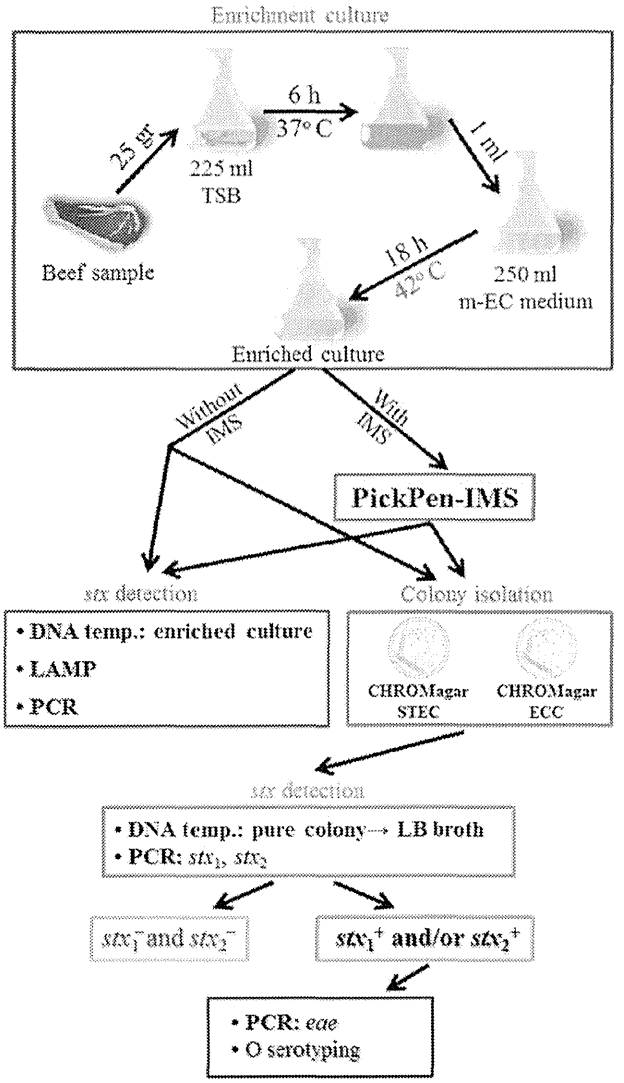

Figure 1: Schematic representation of the protocol for PickPen assisted IMS-LAMP-based detection method for STEC in beef samples.

In the inspection of environmental samples including food, the STEC expressing the known O antigens of EHEC are targeted as a potential public health hazard. Serogroup-specific method and virulence-specific method were combined for detection of STEC belonging to a clinically important O serogroup in some studies. Combinations of simple to sophisticated and high-cost techniques targeting a narrow spectrum of the important O serotypes of STEC/EHEC (a maximum number of eight of target O serotypes). These include multiplex PCR [16], PCR-ELISA and multiplex real-time PCR assays [17] and LAMP [18]; multiplex real-time PCR assays screening for virulence genes and O-antigens encoding genes [15]; immunomagnetic separation (IMS) targeting certain O serotypes of *E. coli* individually or simultaneously [19,20]; and a combination of multiplex real-time PCR and IMS assays [21-23].

Due to the rapid development of transportation, the food trade among various countries has become very active these days. Therefore, specific, sensitive and easy-to-perform methods are necessary for examination of food for a wider range of the important O-serotypes of STEC/EHEC even in resource-limited and tropical countries. In this study, we combined a unique IMS method, as a specific and easy-to-perform, covering clinically important O serotypes worldwide and a loop-mediated isothermal amplification (LAMP) method [24], as a simple, sensitive and low-cost technique, to achieve the goal described above.

Materials and methods

Immunomagnetic beads (IMB)

Magnetic beads were coated with antibodies against seven *E. coli* O antigens using antibodies partially purified from rabbit polyclonal antiserum specific to each of target O antigen (rabbit anti-*Escherichia coli* O157, O26, O91, O103, O111, O121 or O145 antiserum, Denka Seiken Co. Ltd., Tokyo, Japan). These resulted in bead group 1 suspension that targets the O serotypes of clinical importance in Japan. Similarly, bead group 2 suspension containing the beads coated with antibodies against anti- O15, O55, O104, O128 and O153 was prepared. Antibodies against anti- O45, O113 and O118 were unavailable for us and thus were not included. Equal volumes of bead group 1 suspension and bead group 2 suspension were mixed, resulting in the final bead suspension and designated as IMB in this study. This bead suspension (IMB) targets the O serotypes of clinical significance on a global scale. IMB was stored at 4° C and used whenever needed throughout this study.

Beef sample examination

Japanese beef was purchased from 4 local stores in Kyoto City, Japan, in 2013. Malaysian and Thai beef were purchased from a local market in Hat Yai City, southern Thailand, in 2013 and 2014. The protocol used to examine the beef samples is outlined in Figure 1. Twenty five grams of each sample was incubated at 37°C in 225ml of tryptic soy broth (Bacto™ Tryptic Soy Broth; Difco, Becton Dickinson Microbiology Systems, Sparks, MD, USA). After 6 h, 1 ml of the culture was added to 250ml of modified EC medium containing 25mg/l novobicin (Nobobiotin added m-EC medium, Kyokuto Pharmaceutical Industrial Co., Ltd., Tokyo, Japan) and incubated at 42° C for 18 h. The broth culture with or without IMS treatment was examined in two steps. Step 1: the DNA template was prepared by a boiling method: boiling 1ml of the broth culture or bead suspension for 10 min, chilling on ice for 10 min, followed by centrifugation at 15,000 rpm for 5 min and collection of the supernatant. The DNA template was examined for the presence or absence of the *stx* genes by a conventional PCR method as previously described in [25] and the LAMP method according to the instruction by the manufacturer (Loopamp™ Verotoxin-producing *Escherichia coli* Detection Kit, Eiken Chemical Co., Ltd., Tokyo, Japan). Step 2: ten µl of the broth culture or bead suspension was streaked onto two selective agar media and incubated at 37°C for 18 h. Up to 5 suspected colonies from each triplicated agar plate were selected: mauve colonies growing on CHROMagar™ STEC (with 50 mg/l STEC supplement) and blue colonies growing on CHROMagar™ ECC (CHROMagar, Paris, France). The selected colonies were grown in 2 ml of Luria-Bertani broth [26] and the DNA template was prepared and examined by conventional PCR for stx_1 and stx_2 genes. The isolates that gave stx_1^+ and/or stx_2^+ result were examined for the *eae* gene as previously described in [27] and for O serotype by an agglutination test using *E. coli* O antisera (*E. coli* antisera "SEIKEN", Set 1, Denka Seiken Co., Ltd.).

PickPen-Immunomagnetic separation (PickPen-IMS)

A 96-deep well (2-ml capacity) titer plate–based IMS procedure using an eight-channel PickPen device (PickPen® 8-M, BIOCONTROL, Washington, USA) was performed as follows. IMB were placed at the room temperature on a shaker (140 rpm) for 30 min before use. Thirty µl of IMB were mixed with 1 ml of the broth culture in the first well and incubated at the room temperature on a shaker (140 rpm) for 30 min. The PickPen device was applied for 5 min and the captured IMB were transferred to the second well and washed in 1-ml washing buffer [phosphate-buffered saline consisting of 0.01M phosphate and 0.16M NaCl with pH 7.0 (PBS) with added 0.1 % Tween 20]. The washing step was repeated in the third well. Finally, the washed IMB were suspended in 1 ml of the washing buffer in the fourth well (designated as Yeild).

IMS sensitivity

The capture efficiency (CE) % was selected as indicator to evaluate four factors (IMB volume hereinafter referred to as IMBv, incubation

Table 1: Reference strains of *E. coli* used in IMS sensitivity and specificity experiments

Strain name	Origin	Year of isolation	O serotype	Presence of gene:		Literature/source
				stx_1	stx_2	
K-H-1	Human, Korea	1995	O143	–	–	[27]
K-H-2	Human, Korea	1995	O166[1]	–	–	[27]
M47	Beef, Malaysia	1997	OUT[2]	–	–	Laboratory stock
PE-7	Human, Brazil	1989	O126	–	–	[29]
KETE	Human, USA	Unknown	O6	–	–	[30]
KEIE	Human, Thailand	1991-1992	O124	–	–	[31]
EDL993	Human, USA	1982	O157	+	+	[32]
PV11-004	Human, Japan	2011	O91	+	–	Laboratory stock
PV11-006	Human, Japan	2011	O26	+	–	Laboratory stock
PV11-035	Human, Japan	2011	O145	–	+	Laboratory stock
PV10-104	Human, Japan	2010	O103	+	–	Laboratory stock
PV08-103	Human, Japan	2008	O111	+	+	Laboratory stock

[1]Reported as OUT in the indicated literature, but subsequently determined to be O166 by the author (A.Y.K.).
[2]OUT: untypable for O serogroup.

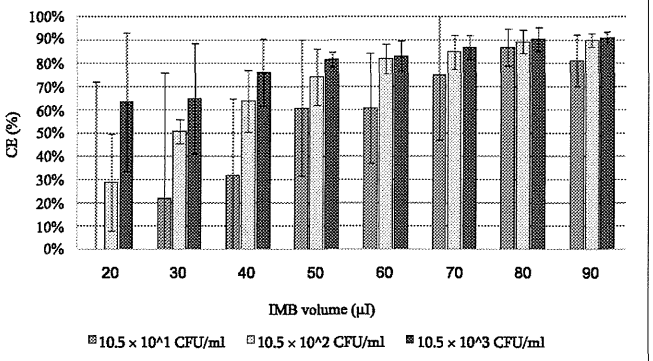

Figure 2: The CE % obtained from three suspensions of the target cell using various volumes of IMB.

Table 2: The result of examination of DNA from enriched culture of beef samples for the *stx* gene purchased in Thailand

Pattern desig.[1]	Result of the *stx* gene detection				No. of beef samples
	Without IMS and by:		With IMS and by:		
	LAMP	PCR	LAMP	PCR	
A	–	–	–	–	26
B	+	–	–	–	7
C	+	–	+	–	28
D	–	–	+	–	11
E	+	+	+	+	1
F	+	+	+	–	1
Total	37	2	41	1	74

[1]Based on the combination of IMS (with or without) and the kind of genetic method (LAMP or PCR) used for detection of the *stx* gene in the enriched culture of the beef sample.

time of the IMB-cell suspension mixture, PickPen application time, and washing step) in IMS sensitivity test. *E. coli* PV10-104 was used in this experiment (Table 1). The strain was grown in Luria-Bertani broth at 37° C for 18 h with shaking (160 rpm). Serial 10-fold dilutions of the culture were made in PBS without Tween 20.

IMBv: one milliliter of cell suspension of each of 10^{-5}, 10^{-6} and 10^{-7} dilutions was mixed with (20 to 90µl) of IMBv. The best IMB volume (bIMBv) was determined.

IMB-target incubation time: four incubation times (5, 15, 30, and 45 min) were tested by incubating 10^{-5} cell suspension of the target cell with bIMBv.

PickPen application time: CE % at selected time points (0.5, 1.5, 3.5, 5, 7 min) of the PickPen application (duration of attracting the IMB by the PickPen) was determined as described below. The CE % relative to the increase in PickPen application time was calculated and the appropriate PickPen application time was determined.

Washing step: 10^{-5} target cell suspension was incubated with the bIMBv for 30 min. The IMB-target cell complex was washed twice and the CE % was determined and the loss of the target cell was calculated.

The CE was calculated as previously described, CE (%) = $(C_0 - C_a)/C_0 \times 100$, where C_0 is the total number of cells present in the sample (CFU/ml), and C_a is the number of cells not bound to IMB (CFU/ml) [28].

The IMS sensitivity (CFU/ml) was defined as the minimum concentration of target cells detectable by IMB at the bIMBv. This was calculated as follows, IMS sensitivity (CFU/ml) = $(C_L \times CE)/100$, where C_L is the low concentration of the examined cell suspensions.

IMS specificity

To evaluate the specificity of the PickPen-IMS used in this study a mixture of *E. coli* strains consisting 6 strains each of targeted and non-targeted O serotypes was treated by this method. After the PickPen-IMS treatment the O serotypes and *stx* genotypes of the *E. coli* remaining in the solution in each deep well of the 96-deep well titer plate were analyzed relative to those of the starting mixture. The details of the experiment are as follows. The twelve *E. coli* strains (Table 1) were grown in Luria-Bertani broth at 37°C for 18h with shaking (160rpm) and the cultures were diluted to 10^{-5}CFU/ml. Equal volumes of each bacterial suspension were mixed in one tube (designated as the starting mix). 20µl of the starting mix was spread on CHROMagar™ ECC in triplicate to screen the starting composition of O serotypes without IMS (as a control). 1 ml of the starting mix was transferred to the first well and mixed with bIMBv, and then PickPen-IMS was performed as described above. The beads were washed in the second and the third wells and finally suspended in the fourth well. Appropriate volumes of the remaining solution in each well were spread on CHROMagar™ ECC in triplicates and incubated at 37°C for 18 h (20, 50, 50, and 20µl, from the first to the fourth well, respectively). Colonies were picked up randomly (up to 24 per plate) and the O serotypes were examined for the selected colonies. DNA templates were prepared from the staring mix and from the solutions remaining in the four wells by boiling and examined by LAMP as described above.

Statistical Analysis

All experiments were conducted in triplicate. The means and standard deviations of all collected data were calculated from independent group of replicates. A Student's t-test was used for statistical analysis of the data between two groups. A p-value ≤0.1 was considered statistically significant.

Results and Discussion

Detection of STEC in the beef samples

In this study, we aimed at developing a specific, sensitive and easy-to-perform detection method for clinically important O serotypes of STEC that can be used in all countries in the world. We examined retailed beef samples (not artificially contaminated) by the procedure outlined

Table 3: Characteristics and isolation procedure and origin of the STEC strains isolated in this study

Strain no.[1]	Beef samples		Pattern[2] desig.	Isolation of *stx*⁺ strains						
				Isolation procedure[3]			Characteristics of the isolated strains			
	Origin	Year of examination		Medium	W/O IMS	W/IMS	O serotype	Presence of gene[4]: stx_1	stx_2	*eae*
AYK1-1	Malaysian	2013	C	S	–	+	O157	–	+	+
AYK2-1	〃	〃	E	S	–	+	O157	–	+	+
AYK3-1	〃	〃	C	S	–	+	O111	+	–	–
AYK4-1	〃	2014	D	S	+	+	O111	+	–	–
AYK4-2	〃	〃	D	S	+	–	O71	+	–	–
AYK4-3	〃	〃	D	S	+	+	O103	+	–	–
AYK5-1	〃	〃	D	S	–	+	O103	+	–	–
AYK6-1	〃	〃	F	E	+	–	O103	+	–	–
AYK7-1	〃	〃	D	S	+	+	O103	+	–	–
AYK8-1	〃	〃	D	S	–	+	O103	+	–	–
AYK9-1	〃	〃	C	S	+	–	O140	+	+	–
AYK10-1	Thai	〃	C	E	+	–	O144	+	+	–

[1]Strains AYK4-1, AYK4-2 and AYK4-3 were isolated from the same beef sample; other strains from different beef samples.

[2]Corresponding to the pattern designation of Table 2 regarding the combination of examination methods for the *stx* gene in the enriched culture of the beef sample.

[3]W/O IMS: without IMS, W/IMS: with IMS, S: CHROMagar STEC, E: CHROM agar ECC, – : not isolated, + : isolated

[4]–: absent, +: present

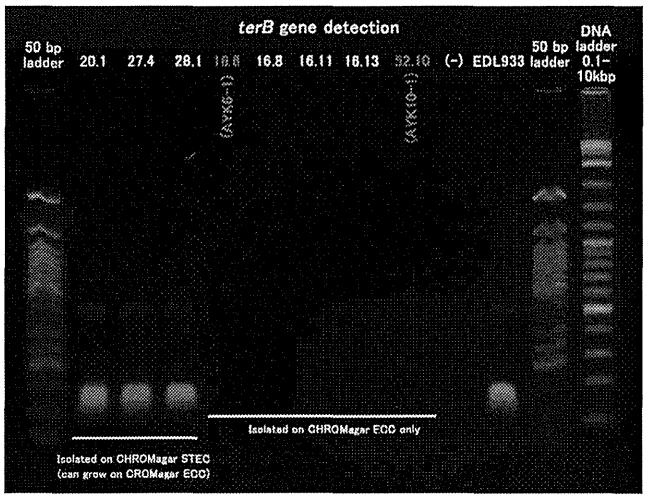

Supplement 1: 16.6: AYK6-1

52.10: AYK10-1

in Figure 1 to evaluate our IMS-LAMP based detection method. We conducted our investigation in Japan and Thailand where distribution of the target bacterium is relatively scarce and prevalent respectively [25,33-35]. In our strategy, initial screening utilized detection of the *stx* gene. We examined not only the boiled supernatant of the enriched culture but also isolated colonies for the *stx* gene in order to check the possibility of false positive and false negative result of the LAMP assay. Twenty-eight Japanese beef samples were examined in 2013. And a total of 74 beef samples (22 and 52 samples, respectively, in 2013 and 2014) purchased in the market in southern Thailand were examined. All 28 Japanese beef samples examined were negative for the *stx* gene with or without IMS treatment. The Japanese result is largely reflecting the high quality and hygienic conditions of beef production in Japan.

The result of the examination for the presence of the *stx* gene in the enriched culture of the 74 beef samples purchased in Thailand was classified into patterns from A to F. This classification is based on the difference in the result obtained by the two genetic detection methods (LAMP and PCR) of the enriched culture treated without or with IMS. Forty-eight (64.9 %) of the 74 samples purchased in southern Thailand gave *stx*⁺ in at least one result of the four categories when enriched beef cultures treated with or without IMS were examined by LAMP and PCR (Table 2). The total number of *stx*⁺ DNA samples obtained by LAMP assay was 26 times (78/3 DNA samples) higher than that obtained by conventional PCR assay.

The 74 beef samples consisted of 35 Thai beef samples and 39 Malay beef samples. 57.1% of the Thai beef and 71.8% of the Malay beef samples gave *stx*⁺ result (data not shown). This result supports the previous report that Malay beef is more frequently contaminated by STEC than Thai beef [33].

In the study in Thailand, we observed two false negative cases of LAMP assay; where LAMP assays gave negative but some isolated colonies gave *stx*⁺ result (Tables 2,3, Pattern D, AYK4-1, AYK4-2, AYK4-3 and AYK7-1, LAMP without IMS). The result may suggest the need for a different DNA template preparation method for the LAMP assay other than the boiling method.

The beef samples classified to Patterns C and D amounted to 39 (52.7 %) beef samples that gave positive result only by LAMP but not by PCR regardless of IMS although *stx*⁺ result could be confirmed for 4 (14.3 %) and 4 (36.4 %) beef samples of Patterns C and D, respectively, by obtaining *stx*⁺ isolates. This result demonstrated how LAMP is more sensitive than PCR and that PCR failed in detecting the *stx* gene in the 8 (Patterns C and D combined) beef samples confirmed by isolation of the *stx*⁺ strains (false negative PCR result). The Pattern D is composed of 11 (14.9 %) samples that gave *stx*⁺ result by LAMP only when IMS treatment was applied, indicating the improvement of the sensitivity by IMS treatment prior to LAMP assay.

However, the Pattern B consists of 7 samples that were positive by LAMP without IMS and turned into negative by LAMP with IMS and we could not isolate any STEC strain which can be explained by a possibility that these 7 samples were contaminated with non-target *E. coli* O serotypes or non- *E. coli* bacteria possessing the *stx* gene [36]. We suspect that the LAMP positive result in Pattern B is most likely to be false positive.

To our surprise, one sample showed Pattern F where STEC O103, one of our target O serotypes, was isolated without IMS but not with IMS; and this particular strain was isolated on CHROMagar ECC only but not on CHROMagar STEC (Tables 2 and 3, AYK6-1). A possible explanation for the first unexpected observation that no STEC was isolated after IMS treatment is that the sample contained a large number of competing populations (*E. coli* expressing target O serotypes but lacking the *stx* gene). Because of abundance of competing population, the total number of STEC O103 after IMS treatment probably became below the detection limit of the PCR assay but was still detectable by the LAMP assay. To explain the second unexpected observation that the strain isolated on CHROMagar ECC was not isolated on CHROMagar STEC (contains potassium tellurite), we investigated the possibility that the isolated strain may lack the tellurite resistance gene (*terB*) [15]. We confirmed this was the case by the PCR assay (Supplement 1).

The selective isolation of STEC through CHROMagar ECC but not CHROMagar STEC was also observed in another case (Table 3, AYK10-1) which was also confirmed to be *terB*$^-$ (Supplement 1). Our result summarized in Table 3 showed that 10 of 12 (83.3%) STEC strains were isolated on CHROMagar STEC but that 2 of 12 (16.7%) STEC strains could be isolated only on CHROMagar ECC. This result is similar to the report by Tzschoppe et al. [15] where 13.6% of EHEC and EHEC-like strains did not grow on CHROMagar STEC. We therefore propose simultaneous use of CHROMagar ECC for the isolation of STEC/EHEC.

In general, we could isolate *stx*$^+$ *E. coli* strains more often from CHROMagar STEC (83.3 %, medium S in Table 3) compared to CHROMagar ECC (16.7 %, medium E in Table 3). Twelve strains belonging to six O serotypes were isolated from 10 beef samples. Nine and one of the ten beef samples were imports from Malaysia into Thailand and domestic product of Thailand, respectively. Of the six O serotypes three (O157, O111 and O103) belonged to the O serotypes of IMS target; two strains of O157 were obtained only with IMS and two strains of O111 and five strains of O103 were obtained with or without IMS. The remaining three O serotypes (O71, O140 and O144) were IMS non-target O serotypes; one strain each of these serotypes was obtained exclusively without IMS. The isolated strains included two O157 strains carrying the stx_2 and *eae* genes; and the other non-O157 strains sharing the stx_1 gene and lacking the *eae* gene (Table 3).

There are the studies reporting isolation of STEC/EHEC belonging to O157 serotype, possessing the stx_2 gene, but producing no or low-level Stx2 from the beef marketed in Hat Yai, southern Thailand [25,33,35]. Sukhumungoon et al. [35] also reported a non-O157 strain carrying the stx_1 gene from the beef purchased in the same mentioned city in Thailand. Their $stx_1$$^+$ non-O157 strain produced a large amount of Stx1. In our study carried out in the same city, we isolated 10 strains of non-O157 STEC and all carried the stx_1 gene. Since this type of non-O157 STEC seems to be prevalent in the beef marketed in this area they may be of public health significance.

Improving IMS sensitivity

The result of the analysis of retail beef samples showed that we could isolate the strains carrying the *stx* gene from 20.8 % of the *stx*$^+$ samples. We explored by in-vitro experiments the possibilities that IMS-LAMP performance can be further improved by fine tuning the factors involved in the IMS. The following four factors were evaluated in details using CE % as the indicator.

IMBv: incubation time of IMB-target cell mixture (30 min) and PickPen application time (5 min) were fixed. The effect of the combination of various concentrations of the target cells (10.5×10^1, 10.5×10^2, and10.5×10^3 CFU/ml) and the various IMBv (20, 30, 40, 50, 60, 70, 80, and 90µl) were compared (Figure 2). The average of the CE % was gradually increased and its standard error was reduced with increase in the IMBv. For comprehensive evaluation of IMBv effect, when the result of CE % of the three concentrations of the target cells were combined, the average ± standard error increased from 25.0 ± 47.3 CE % at 20µl IMBv to 88.4 ± 5.71 CE % at 80µl IMBv. However, increase in the IMBv from 80 to 90µl had no significant effect on the increase of CE % whereas IMBv increase from 70 to 80µl showed significantly increase CE % for the middle and high concentrations of target cell suspension (p=0.1). Therefore, the 80µl of IMBv was judged to be the bIMBv. We found, when IMBv was increased to 80µl or above, the CE value reached a plateau regardless of the cell concentration. Since the ability of IMB to capture the maximum amount of the target cells is limited by the amount of antibodies coating the beads we judged the IMBv of 80µl (bIMBv) is the most suitable for the studies where the concentration of the target cells is unpredictable. The 80µl of IMBv is much more than the volume reported by other workers (20µl) [21,37] and close to the maximum volume that can be handled by the PickPen device in our hands.

Incubation time of IMB-target cell: 2.7×10^3CFU/ml of the target cell incubated with 80µl of IMB were employed. The result (5 min, 13.3 ± 3.5 CE %; 15 min, 70.9 ± 6.9 CE %; 30 min, 90.2 ± 0.4 CE %; 45 min, 86.1 ± 5.1 CE %) showed that the CE % was increased significantly when the incubation time was increased from 5 to 15 min and from 15 to 30 min, but not from 30 to 45 min (p = 0.1). Thus, 30 min incubation time was judged as the required time for the best CE % result.

PickPen application time (duration of attracting the IMB by the PickPen) : 1.1×10^3 CFU/ml of the target cell incubated with 80µl (bIMBv) of IMB were employed. The results (time - CE) were as follows: 0.5 min - 62.1 ± 30.6 CE %; 1.5 min - 57.6 ± 21.7 CE %; 3.5

Table 4: O serotype-based grouping and the number of the colonies randomly selected from the agar plates inoculated with the starting mix (without IMS) and the solution or the suspension remaining in each of the four wells after PickPen-IMS treatment (with IMS).

O serotype-based grouping		Number of the colonies selected[1]:				
		Without IMS	With IMS[2]			
Group	O serotype	(Starting mix)	No wash (First well)	First wash (Second well)	Second wash (Third well)	Yield (Fourth well)
Non-target	O143	–	++++	–	–	–
	O166	–	–	–	–	–
	OUT	+	+++	+	+	–
	O126	++	+++	+	–	–
	O6	++	++	+	–	–
	O124	++	++	–	–	–
	Subtotal	24 (33.3 %)	61 (84.7 %)	4 (26.7 %)	4 (19.0 %)	0 (0 %)
Target	O157	+	+	–	–	+++
	O91	++	–	–	+	++++
	O26	+++	+	–	+	+++
	O145	–	–	+	–	+
	O103	+++	+	+	–	+++
	O111	++	++	++	+++	++
	Subtotal	48 (66.7 %)	11 (15.3 %)	11 (73.3 %)	17 (81.0 %)	72 (100 %)
	Total	72	72	15	21	72

[1]Designations for the number of the colonies: –, 0; +, 1 – 5; ++, 6 – 10; +++, 11 – 15; ++++, 16 – 23.

[2]Designation of the sample solution or suspension is explained in Materials and Methods

min - 65.8 ± 11.6 CE %; 5 min - 83.0 ± 4.73 CE %; 7 min - 61.5 ± 14.2 CE %. P values between the neighboring two time points were: p = 0.44, 0.5 - 1.5 min; p=0.24, 0.5 - 3.5 min; p=0.08, 3.5 - 5 min; p=0.08, 5 - 7 min. The p value was gradually reduced as the time increased, but it appeared to have reached a plateau at 5 min. We therefore judged 5 min is the appropriate application time of PickPen.

Washing step on the loss of IMB-target cell complex in the buffer: the first and the second washing had insignificant effect (p = 0.1) (<1 CE % and <2 CE %, respectively).

After fine tuning of the IMS factors were fixed to as follows, the IMBv to 80µl, incubation time to 30 min, PickPen application time to 5 min and washing step to be repeated twice. These conditions determined the sensitivity of the IMS as 91 CFU/ml at the low concentration of the target cell (Figure 2).

IMS specificity

To evaluate the specificity of the IMS method in vitro, 6 strains of *E. coli* carrying the stx_1 and/or the stx_2 genes, each expressing different target O antigens, were mixed with 6 strains of *E. coli* lacking the *stx* gene and each expressing non-target O antigens. After completion of the IMS treatment, distributions of non-target and target O serotypes in the starting mix (not treated with IMS) and solutions or the cell suspension remaining in the four wells after IMS treatment were examined (Table 4). The result showed that IMS helped to separate and concentrate all target O serotypes (Table 4, Yield). The transition of the change in percentages of target vs. non-target groups showed how and to what extent each step of the PickPen-IMS treatment could contribute to change in the composition of the starting mix. The examination of DNA templates of the 5 suspensions by the commercially available loopamp VT *E. coli* detection kit reflected how LAMP can perform with the help of IMS in this particular experiment as follows: without IMS, no wash, first wash, second wash, and yield, showed respectively, positive, positive, negative, negative, and positive result for the *stx* gene. This result suggests that the remaining target cells in the solutions, first wash and second wash, were below the detection limit of the loopamp kit (60 CFU/test).

We have evaluated the specificity of the IMS by an in vivo assay (Table 3). In the in vivo study of the beef purchased in Thailand, STEC strains belonging to the target and non-target O serotypes were isolated from 8 and 2 LAMP-positive beef samples, respectively. These non-target O serotypes were O140 and O144 (strains AYK9-1 and AYK10-1, respectively, in Table 3), and they were isolated from two different beef samples only without IMS treatment (Table 2, Pattern C). The LAMP positive result with IMS treatment of these samples may or may not be due to these non-target O serotypes. Based on this result, the specificity of the IMS-LAMP detection method can be judged to be very good ranging from 80 % (due to non-target O serotypes) to 100 % (due to target O serotypes). In addition, the IMS was shown to be 100 % specific by an in vitro assay where only target O serotypes were isolated from the Yield (Table 4).

Conclusion

In our current study we designed an IMS-LAMP method targeting as many as twelve O serotypes and to the best of our knowledge, this is the first time to report this number of O serotypes of STEC targeted at once. We have evaluated the specificity of this method by in vivo and in vitro assays and it showed to be 80 to 100 % specific. We regret that we could not include three more O serotypes as the targets of the PickPen-IMS because the antibodies were unavailable when we started this study. However, we have found the antibodies are available recently. The system can therefore be expanded to include the three additional antibodies so that the targets will cover the 15 important O serotypes in the future. We think addition of the antibodies rose to the three or more O antigens, if needed, are possible although the optimal conditions (i.e. bIMBV) and results of the detection method may change. Using a similar PickPen-IMS, our colleagues successfully prepared a set of IMB targeting 69 different K antigens at once and demonstrated its utility by detecting the target organisms from seafood [38]. Therefore, this method may be expanded to include three more O serotypes as a targets totaling to the fifteen O serotypes proposed in the introduction to cover important O157 and non-O157 serotypes in different parts of the world.

Acknowledgments

We are grateful to Kensuke Ozawa, Fumio Gondaira, and Akira Oshima for valuable comments and technical assistance; and to Yohko Takeda, Natthawan Sermwittayawong and Pharanai Sukhumungoon and their graduate students for technical assistance. This research was supported, in part, by Kakenhi Grant-in-Aid for Scientific Research (KAKENHI 24249038) and from the Japan Society for the Promotion of Sciences and a fund for Research on international cooperation in medical science, Research on global health issues, Health and Labour Science Research Grants, the Ministry of Health, Labor, and Welfare of Japan (H26-KOKUI-SITEI-001).

References

1. Farrokh C, Jordan K, Auvray F, Glass K, Oppegaard H, et al. (2013) Review of Shiga-toxin-producing Escherichia coli (STEC) and their significance in dairy production. Int J Food Microbiol 162: 190-212.
2. Nataro JP, Kaper JB (1998) Diarrheagenic Escherichia coli. Clin Microbiol Rev 11: 142-201.
3. Ballmer K, Korczak BM, Kuhnert P, Slickers P, Ehricht R, et al. (2007) Fast DNA serotyping of Escherichia coli by use of an oligonucleotide microarray. J Clin Microbiol 45: 370-379.
4. Stigi KA, macdonald KJ, Tellez-Marfin AA, Lofy KH (2012) Laboratory practices and incidence of non-O157 shiga toxin-producing Escherichia coli infections. Emerg Infect Dis 18: 447–449.
5. Gould LH, Bopp C, Strockbine N, Atkinson R, Baselski V, et al. (2009) Recommendations for diagnosis of Shiga toxin–producing Escherichia coli infections by clinical laboratories. MMWR Recomm Rep 58: 1–14.
6. NIID (National Institute of Infectious Diseases) and Tubeculosis and Infectious Diseases control division, Ministry of Health, labour and welfare, Japan (2012) Symptoms associated with EHEC infection, by serotype. Infectious Agents Surveillance Report (IASR) 33:117.
7. NIID (National Institute of Infectious Diseases) and Tubeculosis and Infectious Diseases control division, Ministry of Health, labour and welfare, Japan (2013) Symptoms associated with EHEC infection, by serotype. Infectious Agents Surveillance Report (IASR) 34: 125.
8. NIID (National Institute of Infectious Diseases) and Tubeculosis and Infectious Diseases control division, Ministry of Health, labour and welfare, Japan (2014) Symptoms associated with EHEC infection, by serotype. Infectious Agents Surveillance Report (IASR) 35: 119.
9. Mathusa EC, Chen Y, Enache E, Hontz L (2010) Non-O157 Shiga toxin-producing Escherichia coli in foods. J Food Prot 73: 1721-1736.
10. EFSA (European Food Safety Authority) (2009) Technical specifications for themonitoring and reporting of verotoxigenic Escherichia coli (VTEC) on animals and food (VTEC surveys on animals and food) on request of EFSA. The EFSA Journal 7: 1–43.
11. Bettelheim KA (2007) The non-O157 shiga-toxigenic (verocytotoxigenic) Escherichia coli; under-rated pathogens. Crit Rev Microbiol 33: 67-87.
12. Johnson KE, Thorpe CM, Sears CL (2006) The emerging clinical importance of non-O157 Shiga toxin-producing Escherichia coli. Clin Infect Dis 43: 1587-1595.
13. García A, Fox JG (2003) The rabbit as a new reservoir host of enterohemorrhagic Escherichia coli. Emerg Infect Dis 9: 1592-1597.
14. De Moura C, Ludovico M, Valadares GF, Gatti MSV, Leite DS (2012) Detection of virulence genes in Escherichia coli strains isolated from diarrheic and healthy feces of dairy calves in Brazil. Arquivos do Instituto Biológico, São Paulo 79: 273–276.
15. Tzschoppe M, Martin A, Beutin L (2012) A rapid procedure for the detection and isolation of enterohaemorrhagic Escherichia coli (EHEC) serogroup O26, O103, O111, O118, O121, O145 and O157 strains and the aggregative EHEC O104:H4 strain from ready-to-eat vegetables. Int J Food Microbiol 152: 19-30.
16. DebRoy C, Roberts E, Valadez AM, Dudley EG, Cutter CN (2011) Detection of Shiga toxin-producing Escherichia coli O26, O45, O103, O111, O113, O121, O145, and O157 serogroups by multiplex polymerase chain reaction of the wzx gene of the O-antigen gene cluster. Foodborne Pathog Dis 8: 651-652.
17. Perelle S, Dilasser F, Grout J, Fach P (2007) Screening food raw materials for the presence of the world's most frequent clinical cases of Shiga toxin-encoding Escherichia coli O26, O103, O111, O145 and O157. Int J Food Microbiol 113: 284-288.
18. Wang F, Jiang L, Ge B (2012) Loop-mediated isothermal amplification assays for detecting shiga toxin-producing Escherichia coli in ground beef and human stools. J Clin Microbiol 50: 91-97.

19. Safaríková M, Safarík I (2001) Immunomagnetic separation of Escherichia coli O26, O111 and O157 from vegetables. Lett Appl Microbiol 33: 36-39.

20. Kanki M, Seto K, Kumeda Y (2014) Simultaneous Immunomagnetic Separation Method for the Detection of Escherichia coli O26, O111, and O157 from Food Samples. J Food Prot 77: 15-22.

21. Fratamico PM, Bagi LK, Cray WC Jr, Narang N, Yan X, et al. (2011) Detection by multiplex real-time polymerase chain reaction assays and isolation of Shiga toxin-producing Escherichia coli serogroups O26, O45, O103, O111, O121, and O145 in ground beef. Foodborne Pathog Dis 8: 601-607.

22. Fratamico PM, Bagi LK (2012) Detection of Shiga toxin-producing Escherichia coli in ground beef using the GeneDisc real-time PCR system. Front Cell Infect Microbiol 2: 152.

23. Madic J, Vingadassalon N, de Garam CP, Marault M, Scheutz F, et al. (2011) Detection of Shiga Toxin-Producing Escherichia coli Serotypes O26:H11, O103:H2, O111:H8, O145:H28, and O157:H7 in Raw-Milk Cheeses by Using Multiplex Real-Time PCR. Applied and Environmental Microbiology 77: 2035–2041.

24. Notomi T, Okayama H, Masubuchi H, Yonekawa T, Watanabe K, et al. (2000) Loop-mediated isothermal amplification of DNA. Nucleic Acids Res 28: E63.

25. Koitabashi T, Vuddhakul V, Radu S, Morigaki T, Asai N, et al. (2006) Genetic characterization of Escherichia coli O157: H7/- strains carrying the stx2 gene but not producing Shiga toxin 2. Microbiol Immunol 50: 135-148.

26. Griffith KL, Wolf RE Jr (2002) Measuring beta-galactosidase activity in bacteria: cell growth, permeabilization, and enzyme assays in 96-well arrays. Biochem Biophys Res Commun 290: 397-402.

27. Kim YB, Okuda J, Matsumoto C, Morigaki T, Asai N (1998) Isolation of an Escherichia coli O157:H7 strain producing Shiga toxin 1 but not Shiga toxin 2 from a patient with hemolytic uremic syndrome in Korea. FEMS Microbiology Letters 166: 43–48.

28. Zeng J, Wei H, Zhang L, Liu X, Zhang H, et al. (2014) Rapid detection of Vibrio parahaemolyticus in raw oysters using immunomagnetic separation combined with loop-mediated isothermal amplification. Int J Food Microbiol 174: 123-128.

29. Tsukamoto T (1996) PCR methods for detection of enteropathogenic Escherichia coli (localized adherence) and enteroaggregative Escherichia coli. Kansenshogaku Zasshi 70: 569–573.

30. Stacy-Phipps S, Mecca JJ, Weiss JB (1995) Multiplex PCR assay and simple preparation method for stool specimens detect enterotoxigenic Escherichia coli DNA during course of infection. J Clin Microbiol 33: 1054-1059.

31. Sethabutr O, Venkatesan M, Murphy GS, Eampokalap B, Hoge CW, et al. (1993) Detection of Shigellae and enteroinvasive Escherichia coli by amplification of the invasion plasmid antigen H DNA sequence in patients with dysentery. J Infect Dis 167: 458-461.

32. Riley LW, Remis RS, Helgerson SD, McGee HB, Wells JG, et al. (1983) Hemorrhagic colitis associated with a rare Escherichia coli serotype. N Engl J Med 308: 681-685.

33. Sukhumungoon P, Nakaguchi Y, Ingviya N, Pradutkanchana J, Iwade Y, Seto K, Radu R, Nishibuchi M, Vuddhakul V (2011a) Investigation of stx2+ eae+ Escherichia coli O157:H7 in beef imported from Malaysia to Thailand. International Food Research Journal 18: 381–386.

34. Ikeda T, Morimoto Y, Tamate N, Shimizu S, Kumada H, Komagome R, Kubo A, Yamaguchi K (2007) Surveillance of foodborne in food. Report of Hokkaido Institute of Public Health 57: 73–75 (article in Japanese).

35. Sukhumungoon P, Mittraparp-arthorn P, Pomwised R, Charernjiratragul W, Vuddhakul V (2011b) High concentration of Shiga toxin 1-producing Escherichia coli isolated from Southern Thailand. International Food Research Journal 18:683–688.

36. Mauro SA, Koudelka GB (2011) Shiga toxin: expression, distribution, and its role in the environment. Toxins (Basel) 3: 608-625.

37. Nou X, Arthur TM, Bosilevac JM, Brichta-Harhay DM, Guerini MN, et al. (2006) Improvement of immunomagnetic separation for Escherichia coli O157:H7 detection by the PickPen magnetic particle separation device. J Food Prot 69: 2870-2874.

38. Tanaka N, Iwade Y, Yamazaki W, Gondaira F, Vuddhakul V, et al. (2014) Most-probable-number loop-mediated isothermal amplification-based procedure enhanced with K antigen-specific immunomagnetic separation for quantifying tdh+ Vibrio parahaemolyticus in molluscansShellfish. Journal of Food Protection 77:1078-1085.

Journal of Food Protection, Vol. 77, No. 7, 2014, Pages 1078–1085
doi:10.4315/0362-028X.JFP-13-536

Most-Probable-Number Loop-Mediated Isothermal Amplification–Based Procedure Enhanced with K Antigen–Specific Immunomagnetic Separation for Quantifying *tdh*$^+$ *Vibrio parahaemolyticus* in Molluscan Shellfish

NATSUKO TANAKA,[1] YOSHITO IWADE,[2] WATARU YAMAZAKI,[3] FUMIO GONDAIRA,[4] VARAPORN VUDDHAKUL,[5] YOSHITSUGU NAKAGUCHI,[6] AND MITSUAKI NISHIBUCHI[6]*

[1]*Graduate School of Medicine and* [6]*Center for Southeast Asian Studies, Kyoto University, Yoshida, Sakyo-ku, Kyoto 606-8501, Japan;* [2]*Mie Prefecture Health and Environment Research Institute, Sakura-cho, Yokkaichi-shi, Mie 512-1211, Japan;* [3]*Department of Veterinary Science, Faculty of Agriculture, University of Miyazaki, Gakuenkibanadainishi, Miyazaki-shi, Miyazaki 889 2192, Japan;* [4]*Denka Seiken Co., Ltd., Nihonbashi-Muromachi, Chuo-ku, Tokyo 103-8338, Japan; and* [5]*Department of Microbiology, Faculty of Science, Prince of Songkla University, Hat Yai 90110, Thailand*

MS 13-536: Received 11 December 2013/Accepted 6 February 2014

ABSTRACT

Although thermostable direct hemolysin–producing (*tdh*$^+$) *Vibrio parahaemolyticus* is the leading cause of seafood-borne gastroenteritis, the enumeration of *tdh*$^+$ *V. parahaemolyticus* remains challenging due to its low densities in the environment. In this study, we developed a most-probable-number (MPN)–based procedure designated A-IS[1]-LAMP, in which an immunomagnetic separation (IMS) technique targeting as many as 69 established K antigens and a loop-mediated isothermal amplification (LAMP) assay targeting the thermostable direct hemolysin (*tdh*) gene were applied in an MPN format. Our IMS employed PickPen, an eight-channel intrasolution magnetic particle separation device, which enabled a straightforward microtiter plate–based IMS procedure (designated as PickPen-IMS). The ability of the procedure to quantify a wide range of *tdh*$^+$ *V. parahaemolyticus* levels was evaluated by testing shellfish samples in Japan and southern Thailand, where shellfish products are known to contain relatively low and high levels of total *V. parahaemolyticus*, respectively. The Japanese and Thai shellfish samples showed, respectively, relatively low (<3 to 11 MPN/10 g) and considerably higher (930 to 110,000 MPN/10 g) levels of *tdh*$^+$ *V. parahaemolyticus*, raising concern about the safety of Thai shellfish products sold to domestic consumers at local morning markets. LAMP showed similar or higher performance than conventional PCR in the detection and quantification of a wide range of *tdh*$^+$ *V. parahaemolyticus* levels in shellfish products. Whereas a positive effect of PickPen-IMS was not observed in MPN determination, PickPen-IMS was able to concentrate *tdh*$^+$ *V. parahaemolyticus* 32-fold on average from the Japanese shellfish samples at an individual tube level, suggesting a possibility of using PickPen-IMS as an optional tool for specific shellfish samples. The A-IS[1]-LAMP procedure can be used by any health authority in the world to measure the *tdh*$^+$ *V. parahaemolyticus* levels in shellfish products.

Vibrio parahaemolyticus, a marine bacterium native in estuarine environments, is potentially pathogenic because some strains carry the *tdh* gene encoding the thermostable direct hemolysin and/or the *trh* gene encoding thermostable direct hemolysin–related hemolysin, which are considered important pathogenicity markers *(13, 21)*. The incidence of *V. parahaemolyticus* infection has increased worldwide since 1996, and this is attributed to the emergence and pandemic spread of a new O3:K6 clone *(16, 25)*. Pathogenic strains can cause gastroenteritis in humans through consumption of contaminated seafood, especially filter-feeding molluscan shellfish, because they concentrate microorganisms from the environment in their digestive tracts *(26)*. This has resulted in efforts to develop methodologies to measure and manage pathogenic *V. parahaemolyticus* levels in shellfish products *(7)*. Nevertheless, due to the low densities of pathogenic *V. parahaemolyticus*, which typically accounts for less than 1% of the total *V. parahaemolyticus* population in the environment *(5, 29, 31)*, the enumeration of pathogenic *V. parahaemolyticus* remains challenging. Today, it is generally accepted that there are very limited cases in which pathogenic *V. parahaemolyticus* can successfully be enumerated by directly analyzing shellfish homogenates; therefore, enrichment is necessary. Consequently, various molecular methods for the detection of total and pathogenic *V. parahaemolyticus* have been applied in a most-probable-number (MPN) format *(2, 15, 17)*. One such MPN-based procedure described by Hara-Kudo et al. *(9)* used conventional PCR in conjunction with a three-step enrichment procedure. This MPN-PCR procedure was later applied in a field setting, the bloody clam risk assessment in Hat Yai, southern Thailand, in which total and pathogenic

* Author for correspondence. Tel: +81-75-753-7367; Fax: +81-75-753-7350; E-mail: nisibuti@cseas.kyoto-u.ac.jp.